Impacts of Different Environmental Forcings and Drought on Grassland Water and Carbon Fluxes

Tristan Green

B.S. Atmospheric Science, University of Kansas, 2019

Submitted to the graduate degree program in Department of Geography and Atmospheric Science and the Graduate Faculty of the University of Kansas in partial fulfillment of the requirements for the degree of Masters of Science.

Dr. Nathaniel Brunsell, Committee Chairperson

Committee members

Dr. Joshua Roundy

Dr. Bing Pu

Date defended: May 7th, 2021

The Thesis Committee for Tristan Green certifies
that this is the approved version of the following thesis :

Impacts of Different Environmental Forcings and Drought on Grassland Water and Carbon Fluxes

Dr. Nathaniel Brunsell, Committee Chairperson

Date approved: May 7th, 2021

Abstract

Vegetation has profound impacts on the local and regional water and carbon cycles. Classifying different environments and analyzing the response to drought allows us to assess the impacts on the water and carbon fluxes. For classifying the different environments, self-organizing maps are utilized using different environmental forcing variables with a land-surface model, Noah-MP. Quantitative statistics and wavelets are used to evaluate the influence that different vegetation cover has on the local and regional responses and temporal dynamics on the water and carbon variables. The heterogeneous vegetation cover impacted the results from the self-organizing maps in demonstrating the local changes in the water and carbon fluxes induced by differences between the model. The wavelets demonstrated that the temporal dynamics of these land covers vary little and tend to have higher coherence with environments the vegetation tend to thrive in. The 2012 drought illustrated the response of the water and carbon fluxes with an extreme event case. During the drought year, a large reduction in precipitation, evapotranspiration, and net ecosystem exchange occurred. However, one year following the drought, a strong increase in evapotranspiration and net ecosystem exchange is shown. Two years after drought the water and carbon fluxes showed to return back to pre-drought conditions. This research increases our knowledge of water and carbon fluxes response to different classified environments and drought impact.

Acknowledgements

I would like to thank all my family, friends, and peers for the encouragement and support throughout. Special appreciation and thanks goes to Dr. Nathaniel Brunsell for the guidance, support, laughs and patience with me throughout my education journey. As well as my committee members Dr. Joshua Roundy and Dr. Bing Pu with their guidance and support. Without them or anyone this research would not have been possible.

Contents

1 Introduction **1**

2 Different Environmental Impacts on Kansas Grasslands using Noah-MP **3**

2.1 Introduction . . . 3

2.2 Methods . . . 5

2.2.1 Study Area . . . 5

2.2.2 NOAH-MP . . . 6

2.2.3 Statistical Framework . . . 7

2.2.3.1 Self Organizing Maps . . . 7

2.2.3.2 Wavelets . . . 9

2.3 Results and Discussion . . . 9

2.3.1 SOM Analysis . . . 10

2.3.1.1 Determination of the Environmental Classes . . . 10

2.3.1.2 Impacts of Environmental Conditions of Water and Carbon Fluxes 13

2.3.2 Wavelet Analysis . . . 21

2.4 Conclusion . . . 27

3 Post-drought Recovery Analysis for Water and Carbon Fluxes in Kansas Grasslands **28**

3.1 Introduction . . . 28

3.2 Methods . . . 30

3.2.1 Study Area . . . 30

3.3 Results/Discussion . . . 31

3.3.1 2012 Drought . . . 31

3.3.2 ET Post-Drought Response . . . 33

3.3.3 *NEE* Post-Drought Response 34
3.4 Conclusion 36

4 Conclusion **39**

List of Figures

2.1 Contributions of each environmental variable for the initial SOM classes (KON left, KFB middle and KFS right). 10

2.2 Displays each of the observations of each class for the variable, $Tair$ [K], across all the years of study for KON. 11

2.3 Distribution of observed and modeled fluxes for site KON. The different panels reflect the water and carbon fluxes, latent heat flux [W m^{-2}] (a), sensible heat flux [W m^{-2}] (b), net ecosystem exchange [μmolCO$_2$ m^{-2} s^{-1}] (c), and gross primary productivity [μmolCO$_2$ m^{-2} s^{-1}] (d). 14

2.4 Distribution of observed and modeled fluxes for site KFB. The different panels reflect the water and carbon fluxes, latent heat flux [W m^{-2}] (a), sensible heat flux [W m^{-2}] (b), net ecosystem exchange [μmolCO$_2$ m^{-2} s^{-1}] (c), and gross primary productivity [μmolCO$_2$ m^{-2} s^{-1}] (d). 15

2.5 Distribution of observed and modeled fluxes for site KFS. The different panels reflect the water and carbon fluxes, latent heat flux [W m^{-2}] (a), sensible heat flux [W m^{-2}] (b), net ecosystem exchange [μmolCO$_2$ m^{-2} s^{-1}] (c), and gross primary productivity [μmolCO$_2$ m^{-2} s^{-1}] (d). 16

2.6 Average Coherency for the site KON. The different panels reflect the water and carbon fluxes, LE (a), H (b), NEE (c), and GPP (d). 23

2.7 Average Coherency for the site KFB. The different panels reflect the water and carbon fluxes, LE (a), H (b), NEE (c), and GPP (d). 24

2.8 Average Coherency for the site KFS. The different panels reflect the water and carbon fluxes, LE (a), H (b), NEE (c), and GPP (d). 25

2.9 Average Coherency plots of LE (a,b,c,d) and GPP (e,f,g,h) of the three sites KON (black), KFB (red), KFS (blue) with the designated classes of Class 1 (a, e), Class 2 (b, f), Class 4 (c, g) and Class 5 (d, h). 26

3.1 Daily Average Air Temperature [K] (a) and Vapor Pressure Deficit [kPa] (b) for the years 2012 (red), 2013 (green), 2014 (blue) and the baseline period (purple). 32

3.2 Cumulative sums of PPT [mm] (dotted) and ET [mm day^{-1}] (solid) for the years 2012 (red), 2013 (green), and 2014 (blue). 33

3.3 Cumulative daily sum of ET [mm day^{-1}] for early growing season (DoY 50-180). For the years 2012 (red), 2013 (green), 2014 (blue) and the baseline period (purple). 35

3.4 Cumulative annual sum of NEE (a) [μmolCO$_2$ m^{-2} s^{-1}], cumulative early growing season (DoY 50-180) of NEE (b), and daily average NEE (c) for the years 2012 (red), 2013 (green), 2014 (blue) and the baseline period (purple). 37

List of Tables

2.1 The root mean squared error (RMSE) between observations and environmental variables for each site and each SOM class. 12

2.2 SOM classes matched across sites with average environmental variables and class condition. 13

2.3 Nash-Sutcliffe Efficiency model agreement values for sensible heat flux (H) [W m^{-2}], latent heat flux (LE) [W m^{-2}], net ecosystem exchange (NEE) [μmolCO_2 m^{-2} s^{-1}], and gross primary productivity (GPP) [μmolCO_2 m^{-2} s^{-1}] of the respected sites and classes. 18

2.4 R-squared model agreement values for sensible heat flux (H) [W m^{-2}], latent heat flux (LE) [W m^{-2}], net ecosystem exchange (NEE) [μmolCO_2 m^{-2} s^{-1}], and gross primary productivity (GPP) [μmolCO_2 m^{-2} s^{-1}] of the respected sites and classes. . 19

3.1 Calculated means and variances for air temperature ($Tair$) [K] and vapor pressure deficit (VPD) [kPa] 32

3.2 Cumulative sums of precipitation (PPT) [mm], evapotranspiration (ET) [mm day^{-1} and net ecosystem exchange (NEE) [μmolCO_2 m^{-2} s^{-1}]. 34

3.3 Early growing season (DoY 50-180) sums for evapotranspiration (ET) [mm day^{-1}] and net ecosystem exchange (NEE) [μmolCO_2 m^{-2} s^{-1}]. 35

Chapter 1

Introduction

Vegetation is an essential variable as it has substantial influence on the local and regional water and carbon cycles. Vegetation directly impacts the water and carbon cycle via altering the stomatal conductance (Collatz et al., 1991), surface characteristics (Sud et al., 1988), and radiative properties (Betts and Ball, 1997; Bonan et al., 2002). The different characteristics of vegetation have dissimilar implications on the land-atmospheric interactions between the local water and carbon dynamics (Quideau et al., 2001; Foley et al., 2000; Weltzin et al., 2003). Furthermore, extreme events can alter the responses of these water and carbon fluxes for different vegetation (Brookshire and Weaver, 2015; Hufkens et al., 2016; Van der Molen et al., 2011). This thesis will analyze how the local water and carbon fluxes are affected by different environments and drought.

Chapter 2 analyzes how different environments impact the water and carbon fluxes of three grassland ecosystems throughout the growing season utilizing a land surface model. Using self-organizing maps (SOMs), we cluster the different environments together using four environmental variables for each site. Once the different environments are classified, quantitative statistics such as root mean square error (RMSE), r-squareds (r2), and Nash-Sutcliffe efficiency (NSE), are used to calculate between the model and observations the water and carbon flux responses to each of the classes. Furthermore, wavelet analysis is used to analyze the temporal dynamics of these fluxes. This analysis provides insight into which specific environments do these ecosystems water and carbon fluxes thrive or break down. Also, it gauges how important heterogeneity between grasslands alters the local water and carbon fluxes pertaining to different local conditions. This chapter further suggests how modeling heterogeneity in land

surface models is necessary when analyzing different grassland cover.

Chapter 3 takes an extreme event case, the drought of 2012, and demonstrates the post drought impacts on the water and carbon fluxes. Major drought events result in a large reduction in precipitation, evapotranspiration, and net ecosystem exchange (Aires et al., 2008; Ripley et al., 2007; Wolf et al., 2016). The response of these variables following the drought are less understood (Yin and Bauerle, 2017; Ruehr et al., 2019; Van der Molen et al., 2011). Here the responses of these variables are noted two years after the 2012 case. This chapter illustrates the recovery time and initial response of evapotranspiration and net ecosystem exchange for one site. As global frequency and intensity of drought is projected to increase (Dai, 2013; Trenberth et al., 2014; Smith et al., 2009) it is essential to evaluate these impacts major drought has on the water and carbon cycle.

These two chapters present the impacts that vegetation has on the local and regional water and carbon fluxes in Kansas grasslands. By allocating to the different environments (Chapter 2) and analyzing the post-drought responses (Chapter 3 of these fluxes, the essential role that vegetation has on the local and regional climate is demonstrated. Additionally, how important vegetation's role is in altering these variables.

Chapter 2

Different Environmental Impacts on Kansas Grasslands using Noah-MP

2.1 Introduction

Vegetation has many impacts on global climate, specifically the water and carbon cycles (Notaro et al., 2006). Vegetation impacts the water and carbon cycle via altering the stomatal conductance (Collatz et al., 1991), directly impacting the carbon assimilation (Thonicke et al., 2001; Jacobson, 2004). Vegetation also alters the surface characteristics via the surface roughness which impacts turbulent transport between the surface and the lower atmosphere and boundary layer dynamics, as well as moisture convergence (Sud et al., 1988). The vegetation alters radiative properties such as albedo (Betts and Ball, 1997), and energy transport via evapotranspiration (Bonan et al., 2002). The type, structure and condition of the vegetation has different implications on the varying climate and regional meteorology (Quideau et al., 2001; Syphard et al., 2018; Camino-Serrano et al., 2014; Williams and Albertson, 2005; Foley et al., 2000; Bonan et al., 2003; Sitch et al., 2003; Fattet et al., 2011; Scott et al., 2006; Weltzin et al., 2003; Knapp and Smith, 2001). Thus, it is important to understand the specific impacts that vegetation type and land cover may have on regional climate.

In the Midwestern and Central Plains there are numerous different land covers and types of vegetation (Pielke et al., 2007; Griffith et al., 2002). This land cover heterogeneity across the Plains leads to changes in local water and carbon dynamics (Brunsell and Anderson, 2011; Raupach and Finnigan, 1995; Lhomme et al., 1994). Specifically, parts of the Central Plains are

experiencing woody encroachment, which is further changing the local climate and weather within the Central Plains (Barger et al., 2011; Huxman et al., 2005; Jackson et al., 2002; Ratajczak et al., 2012, 2011). Land cover heterogeneity combined with woody encroachment instigates changes in the vegetation cover throughout the region. These land cover differences will change the local climate through the alteration of the water and carbon cycles.

Two specific types of land cover that are prominent in the Central Plains are C_3 and C_4 grasses. These vegetation covers each impacts the atmospheric CO2 and temperature (Liu et al., 2015; Wittmer et al., 2010; Randerson et al., 2005). These impacts have distinguishing effects on local climate and agriculture. C_3 vegetation is more prominent in areas with lower temperatures (cooler growing seasons) while C_4 vegetation tends to occur in warmer temperatures (warmer growing seasons) (Liu et al., 2015; Wang et al., 2013). These vegetative differences have clear implications for altering water and carbon fluxes through the maximum rate of photosynthesis, transpiration rate, plant growth rate, and seasonal activity cycles (von Fischer et al., 2008; Wynn and Bird, 2007; Ehleringer and Björkman, 1977; Still et al., 2003). C_3 grasses tend to green up earlier in the spring and fall and are more active under cooler conditions, whereas C_4 grasses are more active during the growing season under much warmer conditions in the mid to late summer (Collatz et al., 1998; Liu et al., 2015; Wagle and Gowda, 2018). Therefore understanding how the water and carbon fluxes are impacted by the local environmental conditions will help understand impacts of future land cover and climatic changes.

Much research has been conducted analyzing the physiological and ecological functions of C_3 and C_4 grasses (Sage and Kubien, 2007; Smith and Freeman, 2006; Taylor et al., 2010; Ricotta et al., 2003). These studies ranged from analyzing the elongated records of C_3 and C_4 vegetation richness and carbon concentrations in different geographical locations (Wang et al., 2013; Manzoni et al., 2011; Sage, 2004). Research has been done analyzing the specific nature of water and carbon fluxes within these grasses (Logan and Brunsell, 2015; Brunsell et al., 2014; Way et al., 2014), however, little research has focused on the behavior of these water and carbon fluxes at different stages throughout the growing season and how the local environmental

conditions directly impact the fluxes.

This study aims to assess the water and carbon fluxes under different environmental conditions throughout the growing season. This will help facilitate our understanding of how ecosystems respond to local and regional environmental changes.

2.2 Methods

2.2.1 Study Area

This study utilizes eddy covariance data from three sites in Northeastern Kansas. The first two eddy covariance sites are located approximately 8 km south of Manhattan, KS at the Konza Prairie Biological Station (KPBS), a long-term ecological research site that enhances studies and research of tallgrass prairie ecosystems. The first is an annually burned grassland watershed (KON). The other site, KFB, has a prescribed burn every four years. This relatively low-frequency of burning has led to an increase in woody encroachment at KFB (Logan and Brunsell, 2015) while KON is dominated by perennial C_4 grass species (*Andropogon geradii, Panicum virgatum, Schizachyrium scopariam, Sorghastrum nutrans*). Since KFB has been experiencing the increase of woody encroachment the soil depths are deeper by about 1-5 m.

The third eddy covariance station is located at the Kansas Field Station (KFS) near Lawrence, KS approximately 115 km east of the two KPBS sites (Brunsell et al., 2014). There is a precipitation gradient between KON to KFS, with annual precipitation ranging from 880 to 980 mm respectively. KFS is a heterogeneous site that is comprised of a mixture of both C_3 and C_4 grasses including *Andropogon virnicus Bromus inermis, Festuca arundinacea, Poa pratensis,* and several other native forbs.

Our goal is to increase our understanding of how the environmental conditions present at each site impact the water and carbon fluxes as well as the capability to accurately model the land-atmosphere interactions. Therefore, we utilize the full data records of each site, which are slightly different; KON data spanned from 2006-2018, KFB spanned 2008-2018 and KFS spanned

2007-2018. In order to characterize the environmental conditions, we used four environmental variables: air temperature (Tair, T_a) [K], wind speed (WS) [m s^{-1}], vapor pressure deficit (VPD) [kPa], and net radiation (Rn) [W m^{-2}]. These four variables were used to classify the environmental conditions utilizing Self Organizing Maps (SOM), described below.

Following the classification of the environment conditions, we analyzed the different flux measurements at each site. We used latent heat (LE) [W m^{-2}], sensible heat (H) [W m^{-2}], gross primary productivity (GPP) [μmolCO$_2$ m^{-2} s^{-1}] and net ecosystem exchange (NEE) [μmolCO$_2$ m^{-2} s^{-1}]. The data were recorded in half-hourly timesteps but were aggregated to daily measurements by either averaging or summation depending on the variable. GPP was calculated using the methods from (Reichstein et al., 2005) for gap filling. Furthermore, the data were filtered to the defined growing season between April 1st to October 1st. This was to ensure that we capture the active period of plant growth. All site data were processed using EddyPro according to Ameriflux standard processing recommendations, see (Brunsell et al., 2014) and (Logan and Brunsell, 2015) for additional details.

2.2.2 NOAH-MP

The NOAH-MP model is a land-surface model that was updated from the original Noah (LSM) with improved dynamics and multiparameterization options (Niu et al., 2011; Yang et al., 2011). The vegetation canopy is confined to the top and bottom of the canopy, crown radius, leaves and prescribed dimensions, orientation, density, and radiometric properties. We used a dynamic vegetation model that allocates carbon to various parts of vegetation throughout the canopy. The canopy stomatal resistance option used the Ball-Berry approach and the two-stream radiative transfer framework applied to vegetative fraction for a simplified radiative budget. The Ball-Berry approach is able to simulate the biotic regulation of evapotranspiration (Bonan et al., 2014). The model was run with hourly timesteps and was aggregated to daily values by either averaging or summation dependent upon the variable. The model was forced with NCEP reanalysis forcing, with a spin up period of three years to initialize the soil moisture

fields. We are not tuning the model to the individual sites and are only using standard options. This was done intentionally in order to assess how the default characterization of model parameters impacts the overall agreement with observations. In particular, this will help us determine how the model operates when simulating different heterogeneous grasslands.

2.2.3 Statistical Framework

We used three analytical approaches in order to investigate the impact of different environmental forcing conditions on vegetation dynamics: self-organizing maps (SOMs), model comparison statistics, and wavelet analysis. The SOMs were used to classify the environmental conditions, then the model performance was assessed using root mean squared error (RMSE), r-squared, and Nash-Sutcliffe Efficiency (NSE). Each of these statistics were calculated for each SOM class and each site.

2.2.3.1 Self Organizing Maps

SOMs are able to capture varying functions and patterns in order to distill different behaviors and dependencies (Hewitson and Crane, 2002). We used self-organizing maps to assess to what extent the model and observations are the same given similar forcing environments. For each site, we constructed the SOM classes using the observed environmental variables. The air temperature, wind speed, vapor pressure deficit, and net radiation were selected as the environmental variables so that we can consistently group conditions as a function of cool/warm, calm/windy, wet/dry and cloudy/clear. Following the classification of each day into an SOM class, we subset the model and observations into the appropriate class to facilitate the analysis of the fluxes and assess model performance for each class.

For the building of the different SOM classes, we used the SOM Kohonen package (Wehrens and Buydens, 2007; Wehrens and Kruisselbrink, 2018). The SOM building routine begins with the SOMs defining a random distribution of nodes (classes) within the data space. Each node is defined by a reference vector of different weighting coefficients of the environ-

mental input variables. For every node, the n-th coefficient in the reference vector will be associated with the number of environmental variables. The distance between each node and the daily environmental variables was calculated using the Euclidean distance. Then the class is selected as the one that minimizes the distance between the input vector and the reference class vector. Each node is then updated with the new input reference vectors that are defined as the process is iterated over the whole dataframe. Here, we used 500 iterations of the dataset to ensure the same weights were determined over each node (Wehrens and Buydens, 2007; Wehrens and Kruisselbrink, 2018). The updates of these weights for the nodes are determined from the 'winning' node and all of its neighbors.

Equation 2.1 represents the equation for the winning node:

$$w_n = w_n + n(t) * g_{in}(t) * (x^d - w_n) \tag{2.1}$$

where w_n is the winning node that uses the learning rate, $n(t)$ to understand how to adjust the weights. $g_{in}(t)$ represents the neighborhood kernel function and x^d represents the Euclidean distance. For more corresponding information please see (Wehrens and Buydens, 2007; Wehrens and Kruisselbrink, 2018)

This process is iterated until there are a certain number of classes defined by each of the reference vectors (Hewitson and Crane, 2002). The number of classes used between all three sites was determined by the Kullback-Leibler (K-L) divergence, which resulted in five classes across the three sites having the lowest mean K-L divergence.

This process results in each day being placed into one of the resulting SOM classes. This will form the basis for our analysis of how grassland ecosystems respond across the different environmental conditions. Since the SOM analysis was conducted independently for each site, we matched SOM classes across sites to the extent possible in order to generalize the SOM results. This facilitates the comparison between the classes across sites.

2.2.3.2 Wavelets

We utilized wavelets to assess to what extent the observed temporal dynamics of the variables were captured by the model. We computed the wavelet spectra for each site and each SOM class to quantify the sensitivity of each class to varying temporal scales. The wavelets were computed using the daily data. In addition to the wavelet spectra, we analyzed the wavelet coherence between the observations and model for each of the flux variables. The wavelet coherence is calculated as (Liu, 1994):

$$\gamma = \frac{(W_1(\lambda, t) * W_2(\lambda, t))}{(|W_1(\lambda, t)| * |W_2(\lambda, t)|)} \tag{2.2}$$

where $W1$ and $W2$ represent the wavelet coefficients of the observations and model respectively, as a function of the scale parameter (λ) and the location parameter (t). We used the Morlet wavelet with a time resolution of one day and had a frequency resolution of 1/20 voices per octave. The coherence was calculated between the model and observations and then averaged across the temporal domain to produce the average coherence. All of the wavelet analysis was conducted using the WaveletComp R package (Rösch and Schmidbauer, 2018).

2.3 Results and Discussion

The SOMs were used to classify the different environmental conditions into classes in order to analyze the implications for the carbon and water fluxes. Following the determination of the classes, we evaluated the observed data and model on the level of agreement using the SOMs and wavelets.

2.3.1 SOM Analysis

2.3.1.1 Determination of the Environmental Classes

In order to facilitate the comparison across sites, we aligned the SOM classes to be most similar in terms of the means and variances as well as the relative weightings of the environmental variables. For example, if we have a high average air temperature and low vapor pressure deficit, we would consider that a warm and dry class. The contribution was determined from the winning weights defined for each class. An illustrative example is shown in Figure 2.1, where class 2 of KFS and class 2 of KON have similar means and variances for each variable and had similar variable dependencies (T_a and WS having small contributions to the class). In addition, the timing of the class within the growing season was taken into account, shown in Figure 2.2. Typically these classes will occur either throughout the whole growing season or the late spring and early fall.

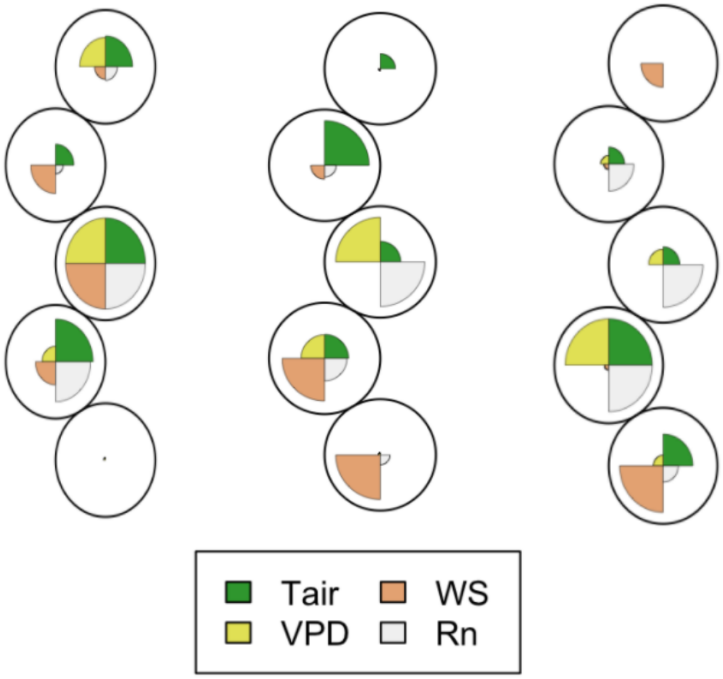

Figure 2.1: Contributions of each environmental variable for the initial SOM classes (KON left, KFB middle and KFS right).

For each class, we calculated the RMSE between the observations and the model for

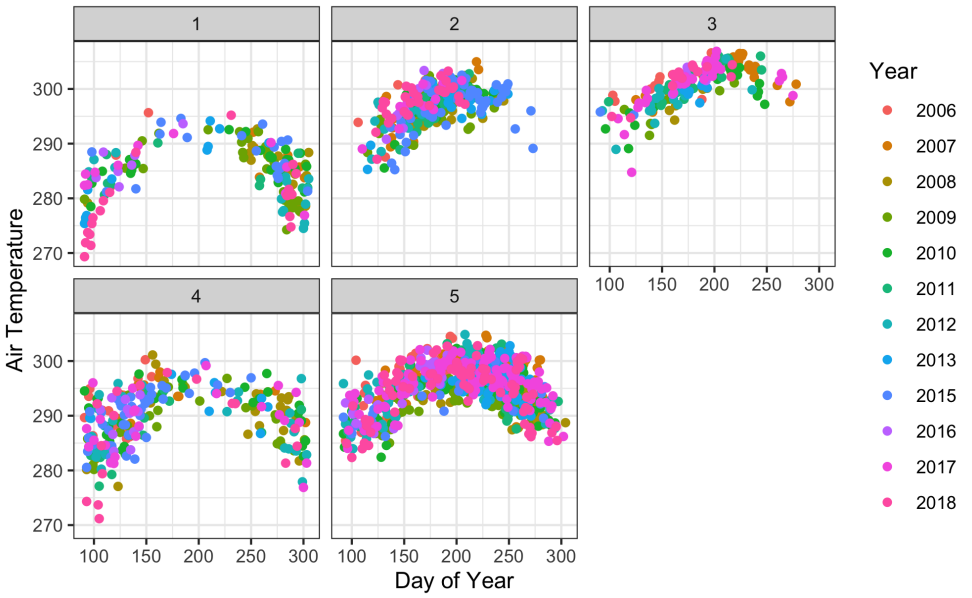

Figure 2.2: Displays each of the observations of each class for the variable, $Tair$ [K], across all the years of study for KON.

each of the environmental variables (Table 2.1). N represents the number of days that were in that class. The RMSEs were only calculated for the environmental variables to understand the differences between the modeling forcing variables for each environmental class. $Tair$ RMSEs ranged from 0.250 to 1.7 K across all the sites and classes. KFB having the smallest RMSEs across all classes being 0.662 K. WS varied between about 1.2 to 2.9 m s[– 1], while VPD ranged from 4.462 to 13.668 kPa. KON had the smallest average WS across all classes being 1.374 m s^{-1} and KFB had the smallest average for VPD of 7.908 kPa. Rn for all classes ranged from about 5 to 49 W m^{-2} with KFS having he smallest average of 25.795 W m^{-2}. These results indicate a consistent evaluation of the environmental forcing data across sites and across class.

Following the determination of the initial classes, we matched the classes from each site into similar environments to facilitate cross-site comparison, Table 2.2. Only if the classes had similar environmental conditions did we match the classes to one another, and classes that could not be matched across sites were not used in the comparative analysis. However, the unmatched classes were still used to assess the overall characteristics of the site. In Table 2.2, "Condition" represents the environment described by the averaged variables for that specific

Table 2.1: The root mean squared error (RMSE) between observations and environmental variables for each site and each SOM class.

Tair [K]	WS [m s^{-1}]	VPD [kPa]	Rn [W m^{-2}]	class -	N -	Site -
1.012	1.483	11.528	49.404	1	260	KON
1.483	1.231	13.668	9.596	2	338	KON
0.665	1.339	8.254	26.353	3	750	KON
0.405	1.271	4.462	16.751	4	196	KON
1.210	1.545	7.592	26.871	5	179	KON
0.250	2.319	6.097	32.072	1	81	KFB
0.713	2.086	12.209	48.436	2	461	KFB
0.740	2.756	6.225	9.275	3	150	KFB
1.033	2.525	7.182	30.840	4	118	KFB
0.573	2.845	7.825	35.109	5	482	KFB
1.006	1.996	9.773	30.956	1	593	KFS
1.256	1.960	7.954	15.323	2	629	KFS
0.716	1.542	9.991	5.562	3	173	KFS
0.523	2.915	9.032	45.552	4	113	KFS
1.575	2.527	9.316	35.584	5	155	KFS

Table 2.2: SOM classes matched across sites with average environmental variables and class condition.

KON	KFS	KFB	Tair	WS	VPD	Rn	Condition
-	-	-	[K]	[m s^{-1}]	[kPa]	[W m^{-2}]	-
1	1	1	288.743	4.403	6.624	84.798	Cool/Windy/Dry/Cloudy
2	2	2	297.816	2.878	13.776	176.540	Warm/Calm/Wet/Clear
4	–	4	299.650	6.048	16.104	154.335	Warm/Windy/Wet/Clear
5	5	–	284.186	2.076	3.576	54.442	Cool/Calm/Dry/Cloudy

class in order to facilitate understanding of the overall class.

2.3.1.2 Impacts of Environmental Conditions of Water and Carbon Fluxes

The distributions of the modeled and observed fluxes for the different sites and environmental classes are shown in Figures 2.3-2.5. For *LE* at KFS the model has a slight over-estimation reflected in the higher distributions across all the classes. This slight over-estimation could be due to the model not accounting for the site receiving more precipitation and thus being slightly more moist (Brunsell et al., 2014). For *H*, the model and observations generally agree across the different environments. The model shows generally larger values (more negative) of *NEE* at KFS. Interestingly, the *GPP* at KFS is captured quite well. The model generally captures the distributions of fluxes at KON and KFB, with the *GPP* being somewhat larger across some (classes 2, 3, and 4) of the different environments. T-tests were run across the distributions of the fluxes for each site not specifically tailoring to each environment. The t-tests indicated that the distributions between the observations and model fluxes were statistically different from one another and the means of each variable were statistically different with p-values generally below 1.759e-15. Only p-value above this was *LE* at KFB which was 0.027.

The r-squared and Nash-Sutcliffe Efficiency (NSE) were calculated between the observed and modeled fluxes, shown in Tables 2.3 and 2.4. The NSE quantifies if the model is capable of capturing the mean behavior. Where if the NSE value is negative, indicates that the mean of the observed variable is a better predictor than the model. A positive value indicates

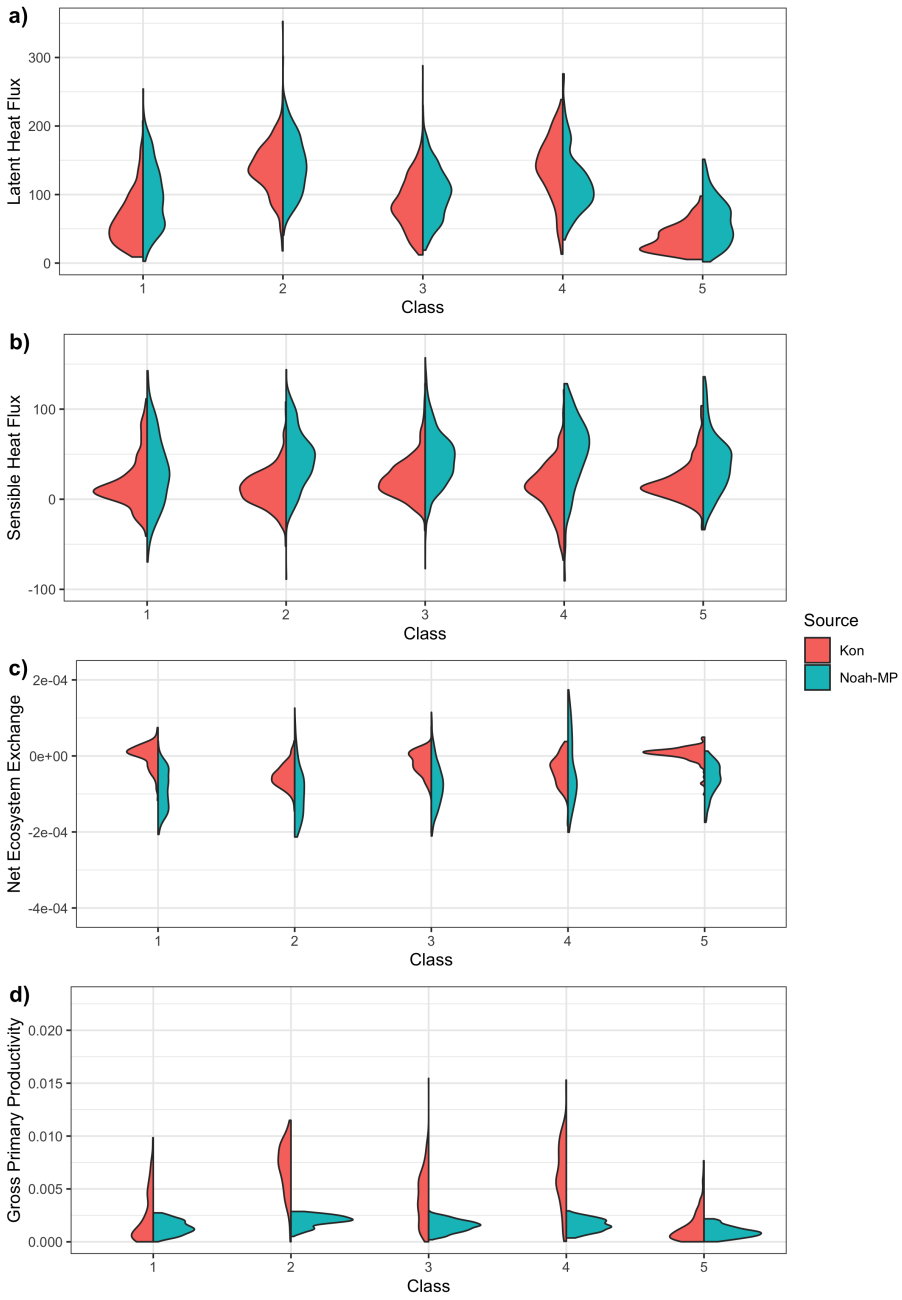

Figure 2.3: Distribution of observed and modeled fluxes for site KON. The different panels reflect the water and carbon fluxes, latent heat flux [W m^{-2}] (a), sensible heat flux [W m^{-2}] (b), net ecosystem exchange [μmolCO_2 m^{-2} s^{-1}] (c), and gross primary productivity [μmolCO_2 m^{-2} s^{-1}] (d).

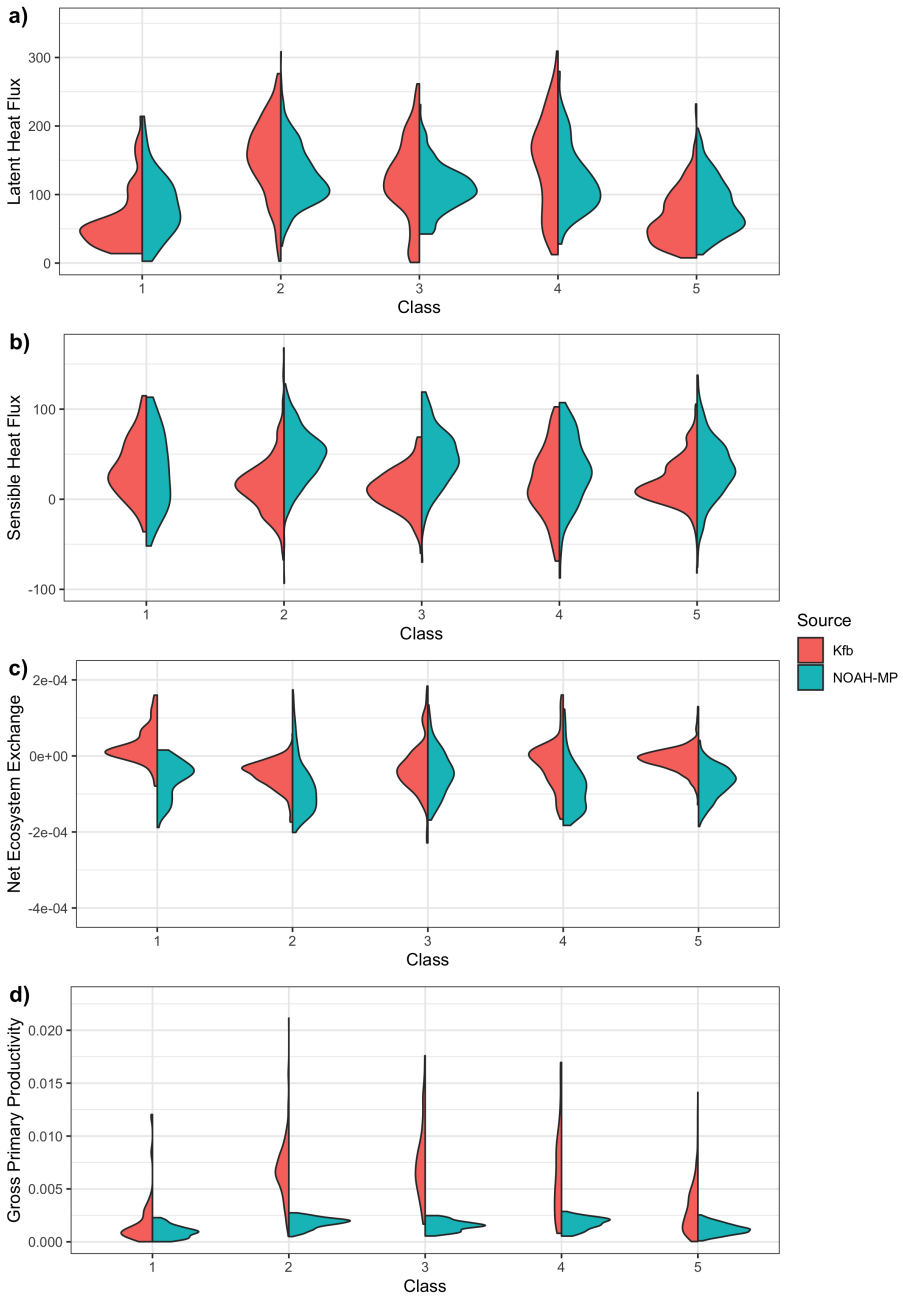

Figure 2.4: Distribution of observed and modeled fluxes for site KFB. The different panels reflect the water and carbon fluxes, latent heat flux [W m^{-2}] (a), sensible heat flux [W m^{-2}] (b), net ecosystem exchange [μmolCO_2 m^{-2} s^{-1}] (c), and gross primary productivity [μmolCO_2 m^{-2} s^{-1}] (d).

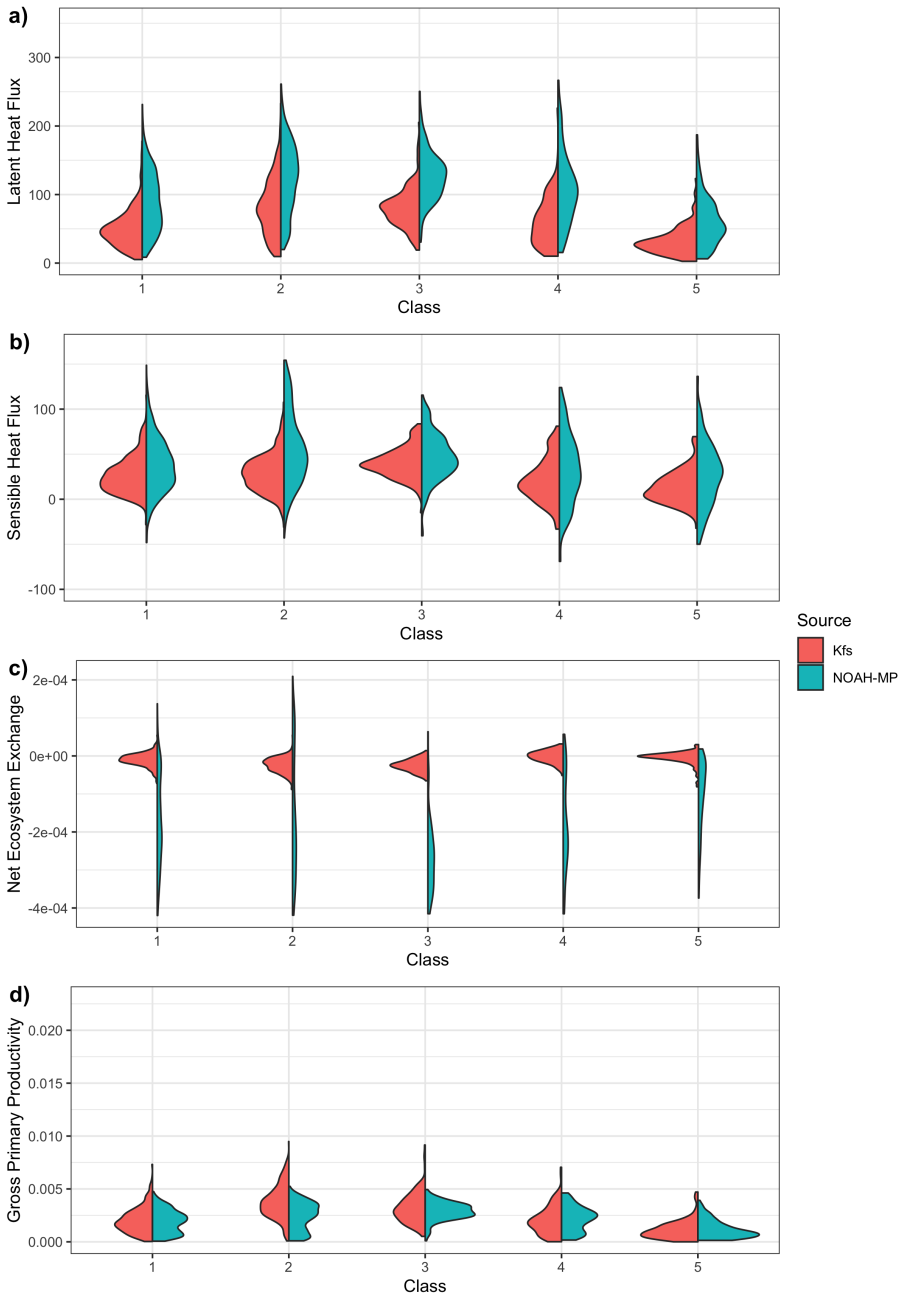

Figure 2.5: Distribution of observed and modeled fluxes for site KFS. The different panels reflect the water and carbon fluxes, latent heat flux [W m^{-2}] (a), sensible heat flux [W m^{-2}] (b), net ecosystem exchange [μmolCO_2 m^{-2} s^{-1}] (c), and gross primary productivity [μmolCO_2 m^{-2} s^{-1}] (d).

that the model is a better predictor than the observed mean. The r-squared value shows if the variance is being captured by the model. Across all sites, for the fluxes we see for the r-squareds that we had relatively low r-squareds across the board (<0.5). This is mostly a result of the model responses in not allocating to the specific sites and being run at base performance. Running at base parameterization was to evaluate the models response to simulating these sites while specifically taking out the heterogeneity forcing of the sites. At KON and KFB, we used classes 1, 2, and 4. In general, KON had higher averaged r-squared values but KFB had higher NSE values across the environmental classes. The r-squared for KON were approximately 0.105 higher for the fluxes. The NSE was higher for KFB being 1.075. For the individual fluxes, H, NEE, and GPP the r-squared values were higher for KON being about 0.114, 0.08, and 0.08. The r-squared for LE was higher for KFB being about 0.04 across all environments. For NSE, H, LE, NEE, and GPP were all approximately 0.55, 1.3, 3, and 0.6 higher for KFB. Based on these results, we can state that the model was better able to capture the variance of the observations at KON, however based on the NSE, the model is more accurate in relation to the means behavior at KFB.

Next, we analyzed the model output for the specific environmental conditions at KON and KFB. For the cool/windy/dry/cloudy conditions (class 1 for each site), we see for the LE at KFB was slightly better than KON in the NSE (~0.86 higher), but has small differences in the r-squared values (~0.06 difference). Similarly for H, we see that the NSE was 0.03 higher for KFB and a small differences of the r-squared of 0.06. The same is found with the carbon variables with KFB having higher NSE values (NSE 2.2 higher for KFB) but KON having higher r-squared (0.2 higher for KON).

In the classes that are characterized as warm and clear days (classes 2 and 4) we see that model captures the means of the water and carbon fluxes better for KFB, shown by the NSE, and captures the variance better for the LE shown by the r-squared. The variance for both the carbon fluxes are better captured at KON. The NSE values at KFB for the LE, H, NEE, and GPP were approximately 0.3, 1.7, 2.1, and 1 higher than at KON. The r-squared values for LE was about 0.05 higher at KFB. H and GPP the r-squareds were about 0.13 and 0.03 higher at

KON, while *NEE* had a difference of 0.0002. For these conditions, the model can capture the means of the water and carbon fluxes better in both the dry and warm environments for KFB. However, it does not capture the variance of these variables. This may be a byproduct of the relationships of each variable at a homogeneous site at KON being easier to capture than the more heterogeneous vegetation cover at KFB.

Table 2.3: Nash-Sutcliffe Efficiency model agreement values for sensible heat flux (H) [W m^{-2}], latent heat flux (LE) [W m^{-2}], net ecosystem exchange (NEE) [μmolCO_2 m^{-2} s^{-1}], and gross primary productivity (GPP) [μmolCO_2 m^{-2} s^{-1}] of the respected sites and classes.

H	LE	NEE	GPP	class	Site
- 0.707	- 1.000	- 8.839	0.171	1	KON
- 3.295	- 0.438	- 5.849	- 4.140	2	KON
- 1.798	- 0.156	- 5.352	- 0.928	3	KON
- 2.424	- 0.288	- 4.118	- 2.229	4	KON
- 1.347	- 2.551	- 13.450	0.243	5	KON
- 0.480	0.034	- 4.408	0.068	1	KFB
- 1.432	- 0.192	- 3.607	- 3.214	2	KFB
- 3.900	- 0.313	- 0.498	- 3.129	3	KFB
- 0.751	0.108	- 1.829	- 1.147	4	KFB
- 1.184	- 0.352	- 4.494	- 0.454	5	KFB
- 1.493	- 3.034	- 128.235	- 0.099	1	KFS
- 4.024	- 1.405	- 121.730	- 0.835	2	KFS
- 1.623	- 2.863	- 273.444	- 0.163	3	KFS
- 1.726	- 2.610	- 195.521	- 0.359	4	KFS
- 2.289	- 3.362	- 56.761	- 0.461	5	KFS

Next, we compare the KON and KFS sites as a function of the environmental class. KON was better captured by the model with regard to both the means (NSE) and variances (r-squared). For the matched classes, we used classes 1, 2, and 5 for each site (Table 2.2). The overall r-squared values between all classes was approximately 0.106 higher for KON. The NSE values were about 0.437 higher (23.829 with NEE) for the fluxes across the compared classes. The largest difference between the r-squared and NSE values occurred in the same environment being the cool/windy/dry/cloudy cluster (class 1). The r-squared was approximately

Table 2.4: R-squared model agreement values for sensible heat flux (H) [W m^{-2}], latent heat flux (LE) [W m^{-2}], net ecosystem exchange (NEE) [$\mu molCO_2$ m^{-2} s^{-1}], and gross primary productivity (GPP) [$\mu molCO_2$ m^{-2} s^{-1}] of the respected sites and classes.

H	LE	NEE	GPP	class	Site
0.277	0.388	0.263	0.488	1	KON
0.205	0.133	0.023	0.131	2	KON
0.155	0.261	0.084	0.338	3	KON
0.171	0.193	0.040	0.181	4	KON
0.294	0.249	0.058	0.448	5	KON
0.213	0.395	0.010	0.320	1	KFB
0.073	0.168	0.057	0.108	2	KFB
0.020	0.005	0.037	0.010	3	KFB
0.027	0.253	0.010	0.140	4	KFB
0.105	0.187	0.007	0.252	5	KFB
0.143	0.250	0.034	0.160	1	KFS
0.093	0.248	0.037	0.119	2	KFS
0.107	0.187	0.018	0.039	3	KFS
0.125	0.243	0.073	0.053	4	KFS
0.339	0.193	0.012	0.057	5	KFS

0.207 higher for KON and the NSE was 1.028 higher (59.801 with NEE) as well. When comparing the r-squared values between the water and carbon fluxes there are striking differences between the environments. For *LE* across the overall environments the difference of r-squared values is only 0.013 whereas for the carbon fluxes it's 0.165. *H* had a large difference of r-squared being ~0.19 higher for KON.

For the carbon variables both the cool, dry, and cloudy environments (classes 1 and 5) had the largest discrepancies between the r-squared values (approximately 0.276 and 0.165, respectively). Whereas the warm environment (class 2) had small differences for the carbon fluxes (~0.001). The NSE did not have large differences across the fluxes between the different environments. With KON having better results for both the r-squared and NSE, we see that the model performs better in this grassland than at KFS. Furthermore, for the different environments, the water fluxes have less differences compared to the carbon fluxes, especially in the cooler environmental conditions (classes 1 and 5). These results may be due to the model being more suitable at the more homogeneous C_4 vegetation cover represented at KON than the more heterogeneous grassland cover at KFS (a mixture of C_3 and C_4 vegetation types) (Brunsell et al., 2014).

The next site comparison is between KFS and KFB. Overall, there were small differences in the r-squared values, but the NSE values were higher at KFB. For the matched classes at these sites, we focus on classes 1 and 2 (Table 2.2). The overall r-squared values for the fluxes were ~0.033 higher at KFB. While the NSE were ~30.975 higher at KFB for each environmental class. For the specific environments, the cool/windy/dry/cloudy environment (class 1) had the largest difference between the two sites for all of the fluxes. The water and carbon fluxes had r-squared values about 0.145 and 0.068 higher for KFB. *H* was ~0.07 higher at KFB. The *LE* had an NSE value about 3 higher and *H* was ~1 higher at KFB. The warmer/calm/wet/clear environment (class 2) had the smallest variability between the fluxes for the r-squared being approximately 0.07 (*LE*), 0.02 (*H*), and 0.001 (carbon fluxes) apart (NSE for *LE* being ~1.2 higher at KFB). This demonstrates that the model performed better at KFB specifically in the cooler, windy, dry, and

cloudy environment than a warm, calm, wet, and clear environment. Overall, these statistics indicate that modeled fluxes performed better at KFB than KFS.

We find that overall the model performed better at KON and KFB than KFS. This may be a byproduct of the model being more applicable in homogeneous grasslands than heterogeneous grasslands (Schmid, 2002). KON is a C_4 grassland, while KFB is a C_4 grass invaded by C_3 woody species and KFS is a mixture of C_3 and C_4 grasses. We see at KFB, the model simulated the *LE* better in each environmental class than at the other two sites. However, the model under performed with respect to both the carbon fluxes at this site compared to KON. This suggests that the model is not accurately simulating the carbon dynamics of woody encroachment. This is illustrated with the strong variability between the carbon fluxes in each class comparing to the other sites.

Furthermore, we find that using Noah-MP's base parameterization scheme and not tuning the model to the specific sites impacted the ability of the model under certain conditions. In particular, the model was unable to capture the distribution of NEE at KFS under most environmental conditions as represented by the NSE. The relatively low r-squared values and NSEs for most of the fluxes illustrate how the model struggles to capture the mean and variances of the fluxes at each site under different environmental conditions. Within the context of applying the model in an operational context, these results suggest further efforts are necessary in parameterizing the heterogeneous vegetation assemblages present in the central U.S.

2.3.2 Wavelet Analysis

Next, we examined how the model was able to characterize the temporal dynamics relative to the observations at each site. By applying a wavelet analysis to the different environmental classes we were able to more fully characterize the impacts of the different environments. Figures 2.6-2.8 illustrates the average coherence of the three sites and Noah-MP for LE, H, NEE, and GPP respectively. These figures display the strong signal of the diurnal (period of 1), seasonal (period of 128), and annual (period of 365) components with the average coherence being

close to one between the model and observations. An average coherency of one demonstrates that the model and observations are perfectly in sync with respect to the coherency. By subsetting the wavelet coefficients to the different classes, we see that the relationships between the different periods illustrate the ability of the model to capture the different temporal dynamics of temperature at each site. This is shown by the relatively high coherency (>0.7) throughout, Figures 2.6-2.8, for each specific panel illustrating each variables average coherency for each site.

When evaluating between the different environments of the fluxes we see that there is a high level of coherency between all of the sites at the diurnal to seasonal scales. There is not much variability between the environments and variables across each site at this frequency. However, we start to see deviation between the different environments and variables at timescales longer than the seasonal scale. At KFB, for LE and GPP show differences at the annual frequency between the cool/dry (class 1) and warm/wet (classes 3 and 4) environments. We see for the cooler drier environment that LE and GPP have a higher coherency (>0.95) than the warmer environments (~0.82). Furthermore, for class 1 for both LE and GPP at higher seasonal period KFB has much higher average coherency than the other two sites (~0.82) (Figure 2.9). This contrast may be related to the model capturing the better environments suitable for C_3 grasses, whereas performing less well under the warmer/wet conditions. For the other two sites, there is little difference between the other classes seen throughout the changing periods.

These results illustrate that across all sites and variables, the model is able to systematically capture the same temporal dynamics. The model routinely captures the strength in signal between the different variables on a diurnal, seasonal, and annual for the fluxes. Furthermore, the differences between the warmer and cooler environments of the LE and GPP at KFB highlight how the model is able to capture the responses to where these ecosystems tend to thrive in. This difference between the environments further illustrates the importance of defining vegetation and parameterizing the model, which has implications for the routine application of this type of model in these heterogeneous vegetation covers that are not easily represented by single

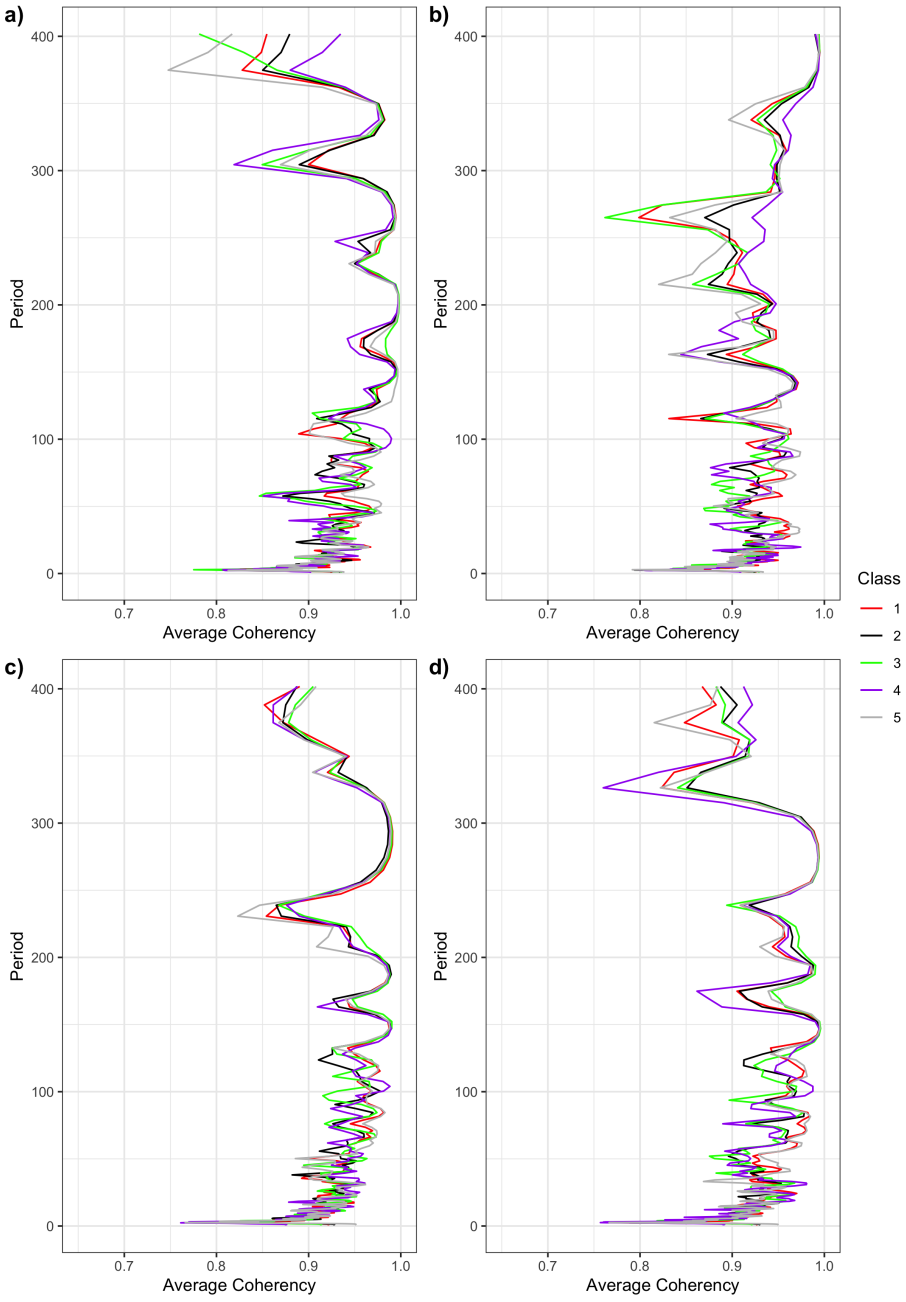

Figure 2.6: Average Coherency for the site KON. The different panels reflect the water and carbon fluxes, LE (a), H (b), NEE (c), and GPP (d).

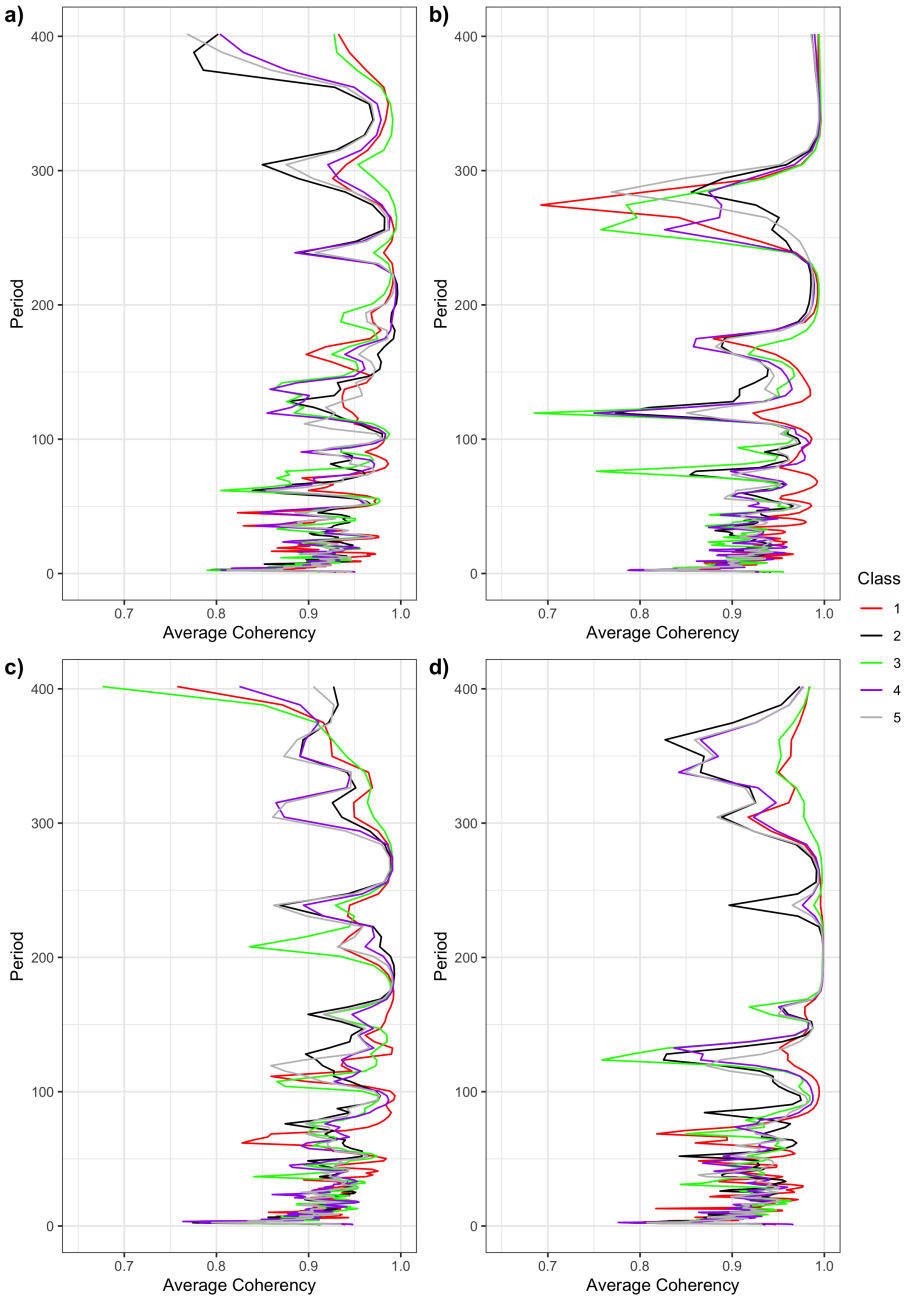

Figure 2.7: Average Coherency for the site KFB. The different panels reflect the water and carbon fluxes, LE (a), H (b), NEE (c), and GPP (d).

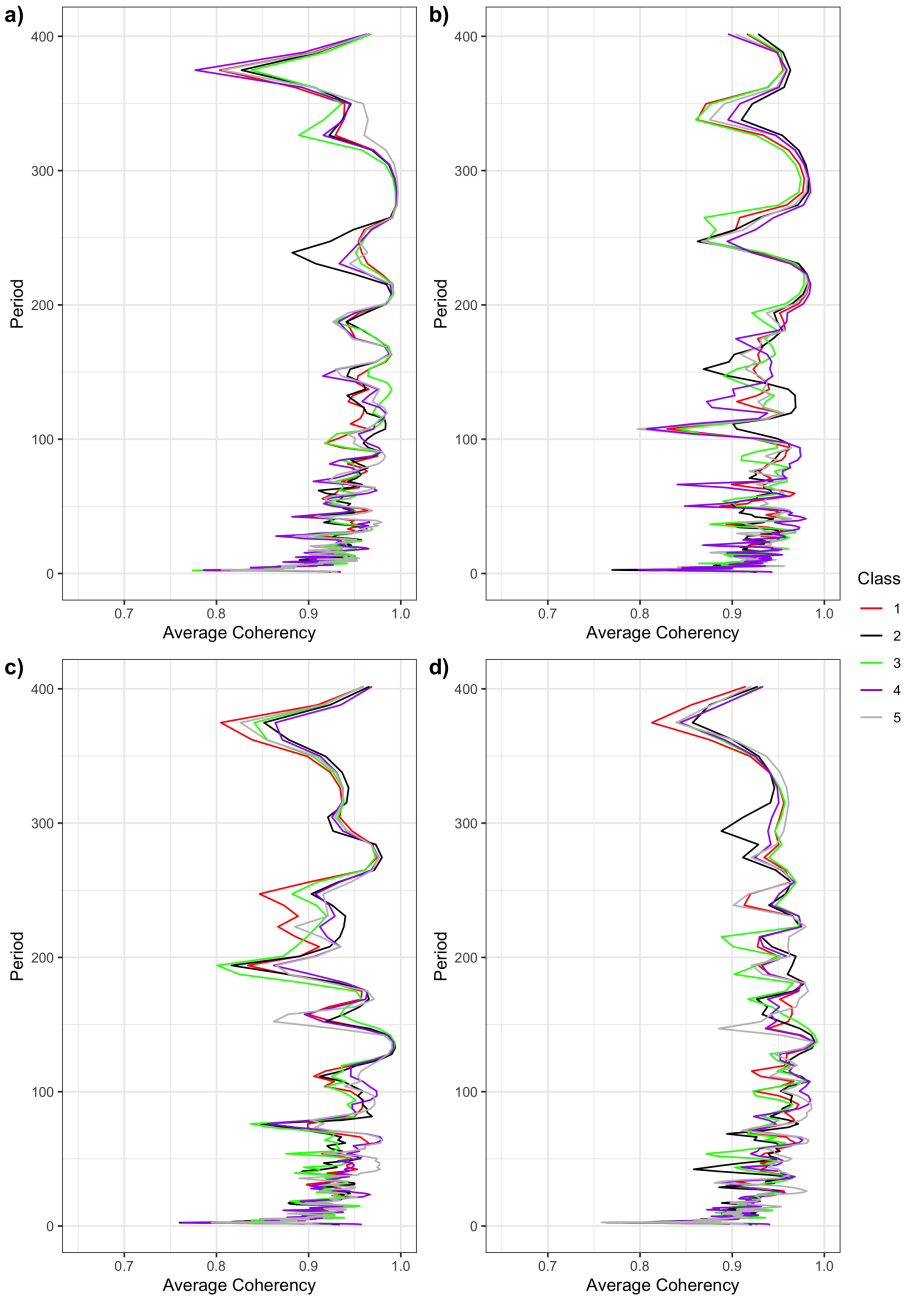

Figure 2.8: Average Coherency for the site KFS. The different panels reflect the water and carbon fluxes, LE (a), H (b), NEE (c), and GPP (d).

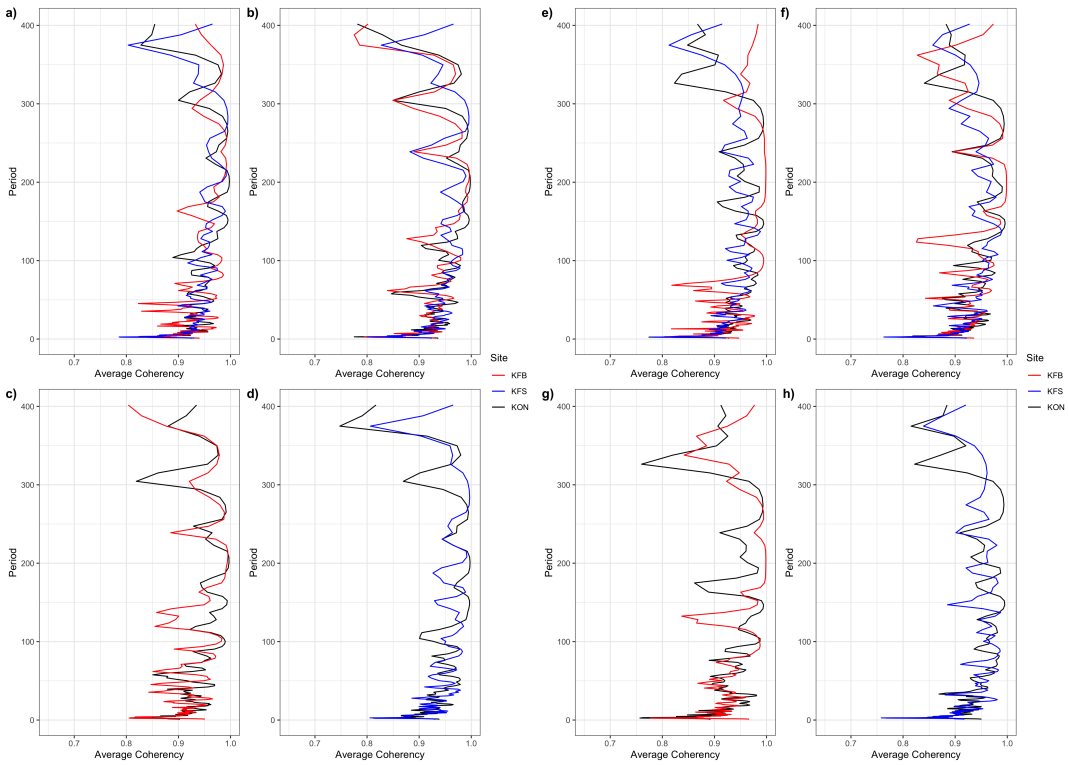

Figure 2.9: Average Coherency plots of LE (a,b,c,d) and GPP (e,f,g,h) of the three sites KON (black), KFB (red), KFS (blue) with the designated classes of Class 1 (a, e), Class 2 (b, f), Class 4 (c, g) and Class 5 (d, h).

vegetation classes.

2.4 Conclusion

The vegetation dynamics across Kansas grasslands can be seen to be mostly similar, however have small differences induced by the heterogeneity of vegetation cover. The SOM results were able to distinguish between the different environments and demonstrate the importance of the different grassland species to the water and carbon fluxes. The Noah-MP model was able to simulate the variations in the water and carbon fluxes. However, the model under performed when capturing the distributions of the water and carbon fluxes for the more heterogeneous grasslands. The wavelet analysis showed that the temporal dynamics of the fluxes were similar across the different frequencies. The model was able to capture the temporal distributions of the carbon and water variables of the three sites. However, KFB exhibited differences between the cool and warm environmental classes with the cool class performing better than the warmer environments which may highlight conditions of which these grasslands tend thrive in (Wang et al., 2013; Liu et al., 2015).

The implications of this work shows the importance of understanding the different water and carbon fluxes when analyzing both homogeneous and heterogeneous grasslands. Under global climate change conditions, it is expected that these grasslands will respond differently when subjected to different environmental forcings. Therefore, it is essential that we are able to simulate these potential responses. This paper suggests some areas of improvement are necessary when examining model responses to these different conditions.

Chapter 3

Post-drought Recovery Analysis for Water and Carbon Fluxes in Kansas Grasslands

3.1 Introduction

The frequency and intensity of drought is projected to increase with the intensification of warmer temperatures in the 21st Century (Dai, 2011, 2013; Trenberth et al., 2014). This projection of warmer and longer droughts will likely have substantial impacts on climate, weather, agriculture, and other sectors. Previous work has shown the underlying impacts of this prolonged and more intense projection of drought and other climate extremes (Easterling et al., 2000; Hoover et al., 2014; Smith et al., 2009). Specifically how drought and other climate extremes affect global and U.S. grasslands (Brookshire and Weaver, 2015; Dreesen et al., 2012; Haddad et al., 2002; Hufkens et al., 2016; Van der Molen et al., 2011). Climate and vegetation elements such as the carbon cycle (Arnone et al., 2011), biomass (De Boeck et al., 2010), vegetation richness (Breshears et al., 2005) are all sensitive to the impacts of climate extremes and drought for grasslands.

As the intensity of climate extremes is expected to increase with projected warmer global temperatures (Smith et al., 2009), ecosystems and biomes will continue to approach unknown regions of the climate space (Shi et al., 2014). Furthermore, the effects of climate extremes on vegetation vary between each ecosystem and local climate (Breshears et al., 2005, 2009; Hanson and Weltzin, 2000; Vicente-Serrano, 2007; Wolf et al., 2014; Teuling et al., 2010). This opens the possibilities of many questions in climate extremes on all types of vegetation. Of the climate extremes, droughts play a major role in the reduction in ecosystem function and

productivity in native grasslands (Hoover et al., 2014; Al-Kaisi et al., 2013). Drought is a major constraint limiting crop production, photosynthesis, and reducing water use efficiency in plants (Farooq et al., 2012; Meir et al., 2008). The intensity and duration of droughts are projected to increase due to climate change (Fischer and Schär, 2009; Vidale et al., 2007; Swann, 2018), therefore, understanding the impacts of drought on vegetation, specifically the water and carbon fluxes is essential.

C_4 grasses play a major role in global climate, biofuels, and agriculture (Still et al., 2003; Taub, 2000; Heaton et al., 2008; Sage, 2004). Much research has been conducted on drought impacts on C_4 grasslands (Aires et al., 2008; Ripley et al., 2007; Vanaja et al., 2011; Carmo-Silva et al., 2008; Heckathorn and DeLucia, 1994; Ghannoum, 2009), specifically native C_4 grasses have shown strong responses to different induced periods of drought (Killi et al., 2017; Taylor et al., 2011; Ripley et al., 2010; Ghannoum et al., 2002). This research (Ripley et al., 2007; Vanaja et al., 2011; Taylor et al., 2011; Ghannoum et al., 2002; Carmo-Silva et al., 2008) focused on analyzing the impacts of the water and carbon fluxes to the initial disturbance until the end of the drought period. However, little research has been conducted analyzing the response of these water and carbon fluxes for the subsequent years after drought (Yin and Bauerle, 2017; Ruehr et al., 2019; Van der Molen et al., 2011). We are interested in the response post-drought of the water and carbon fluxes to return to their pre-drought state specifically with the 2012 drought.

The 2012 drought was noted as a major precipitation deficit and net carbon decrease across the majority of the Central US (Boyer et al., 2013; Rippey, 2015). The effects of this specific drought on the environment and are noted in research (Boyer et al., 2013; Rippey, 2015; Wolf et al., 2016), however little has shown the effects post-drought water and carbon fluxes for the years after the event. Here we show the effects of the 2012 drought on evapotranspiration (ET) and net ecosystem exchange (NEE) as well as the impacts post-drought in 2013 and 2014 using eddy covariance data. This study further demonstrates the strong impact that drought has on the precipitation, water, and carbon fluxes and the post-drought response of the water and carbon fluxes.

In this paper, we will examine the 2012 drought in the Central U.S. and analyze the recovery of the water and carbon variables back to their pre-drought conditions in a C_4 grassland. By analyzing the impacts of this specific drought on the water and carbon cycling, this will further our understanding of the responses to extreme events and their recovery post-drought.

3.2 Methods

3.2.1 Study Area

This study utilizes an eddy covariance site located in Northeastern Kansas that is approximately 8 km south of Manhattan, KS. The Konza Prairie Biological Station (KPBS) is a long-term ecological research site that enhances studies and research of tallgrass prairie ecosystems that monitors the eddy covariance site (KON). KON experiences a mid-continental climate with warm, wet growing season (mean growing season temperature of of 20.8 C and rainfall of 586 mm) and a cool, dry winter (winter temperature is 4.3 C with a rainfall of 224 mm). KON is an annually burned grassland watershed which consists of native C_4 tall grass (*Andropogon geradii, Panicum virgatum, Schizachyrium scopariam, Sorghastrum nutrans*).

Our goal is to increase our understanding of how drought impacts the water and carbon fluxes and the recovery following the event. We utilized the data from 2006-2014. We used latent heat flux which was converted to evapotranspiration (ET) [mm day^{-1}] and net ecosystem exchange (NEE) [μmolCO$_2$ m^{-2} s^{-1}] for the desired fluxes. Furthermore we used air temperature $Tair$ [K], vapor pressure deficit VPD [kPa] and precipitation (PPT) [mm]. The data were recorded in half-hourly timesteps, but were aggregated to daily measurements by averaging each variable. For ET we note the number of days missing data, 2012 (121 days), 2013 (86 days), 2014 (74 days). NEE had no days of missing data for all years. This site datum were processed using the EddyPro software according to Ameriflux standard processing recommendations, see (Brunsell et al., 2014) and (Logan and Brunsell, 2015) for additional details. We defined the pre-drought baseline for each variable from the average of the data record prior (2006-2011) to the

drought event (2012). This allowed us to compare these variables to the pre-drought event and recovery back to the values represented by this baseline period.

3.3 Results/Discussion

3.3.1 2012 Drought

The 2012 drought was a noted as a major precipitation deficit and net carbon decrease across the majority of the Central US (Boyer et al., 2013; Rippey, 2015). This is confirmed with our site from analyzing the deficit of annual sum of PPT, ET, and NEE from the baseline period, shown in Table 3.2. For PPT our pre-drought period calculation for the year was 874.5 mm, ET was 728.3343 mm day^{-1}, and NEE was -0.00131 μmolCO$_2$ m^{-2} s^{-1}. We saw a reduction of all variables in 2012 with KON receiving 568.9 mm of PPT, 405.7975 mm day^{-1} of ET, and -0.00031 μmolCO$_2$ m^{-2} s^{-1} of NEE. These reductions of these variables demonstrates the effects that the 2012 drought had on one site compared to its pre-2012 conditions.

Air temperature and vapor pressure deficit shows little variation between the subsequent years from the pre-drought period to the end of 2014. Figure 3.1 and Table 3.1 shows the air temperature and vapor pressure deficit for the baseline and 2012-2014. We find that the mean difference for temperature across all years is relatively small (1.03 K) with the largest difference occurring in 2014 (2.0520 K) and smallest in 2013 (0.3904 K). For VPD, we find the mean difference to be small as well (1.06 kPa) with the largest difference occurring in 2012 (1.8025 kPa) and the smallest in 2013 (0.5209 kPa). Furthermore, paired t-tests were ran between the baseline and subsequent years of which they have similar significance in relation to the means ($p<0.02$). We demonstrate that from the environmental conditions, there was not any notable changes from our pre-drought baseline period to the subsequent years. When considering the post-drought response, we find that with little change to environmental variables from the pre-drought period, that the environmental conditions factor much less into the observed behavior of the water and carbon variables.

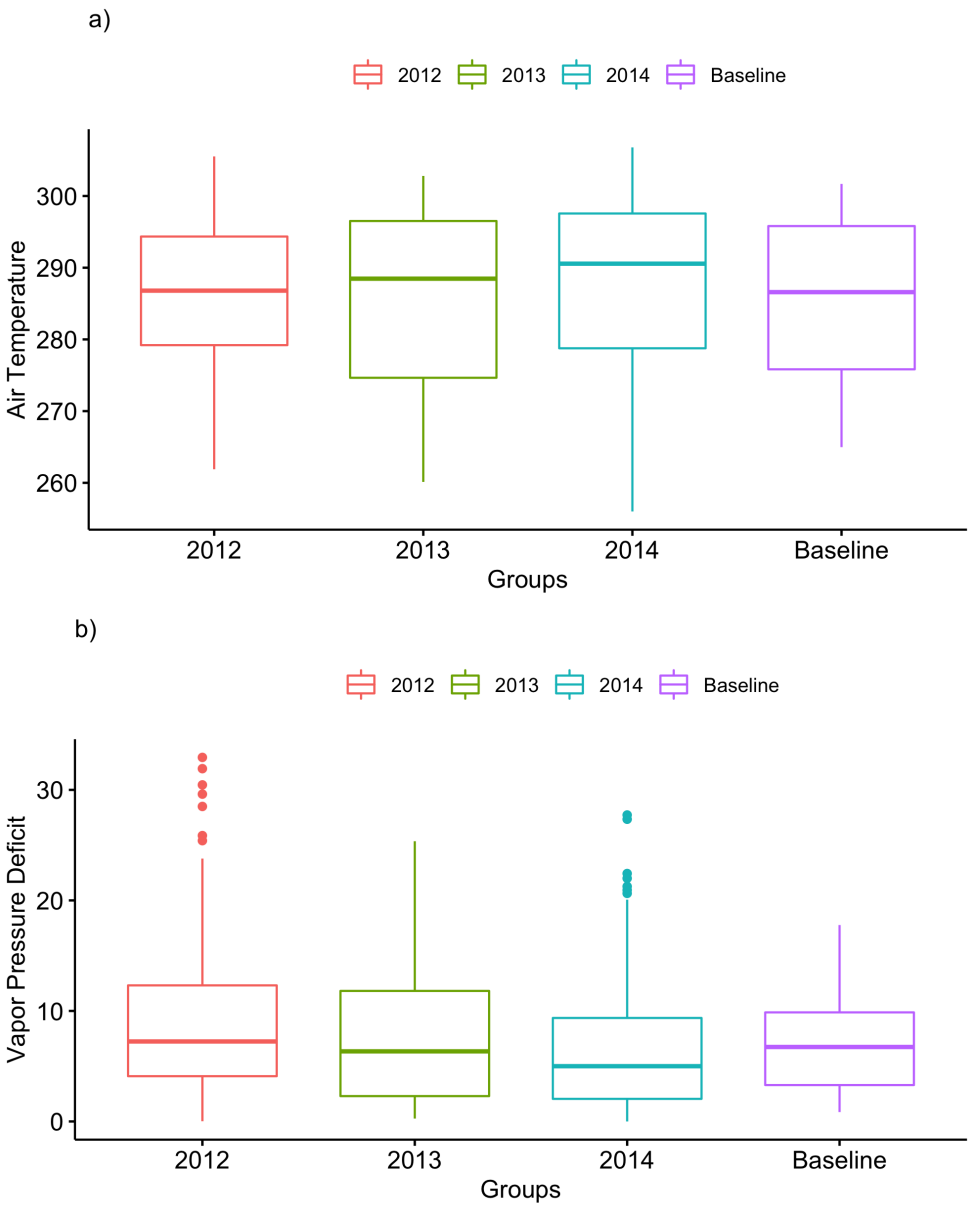

Figure 3.1: Daily Average Air Temperature [K] (a) and Vapor Pressure Deficit [kPa] (b) for the years 2012 (red), 2013 (green), 2014 (blue) and the baseline period (purple).

Table 3.1: Calculated means and variances for air temperature ($Tair$) [K] and vapor pressure deficit (VPD) [kPa]

Var	Stat	Baseline	2012	2013	2014
$Tair$	Mean	285.7239	286.3776	285.3335	287.7768
$Tair$	Variance	105.6814	91.2111	144.1766	143.9821
VPD	Mean	7.0184	8.8209	7.5393	6.1670
VPD	Variance	16.9468	42.2346	34.3155	27.2826

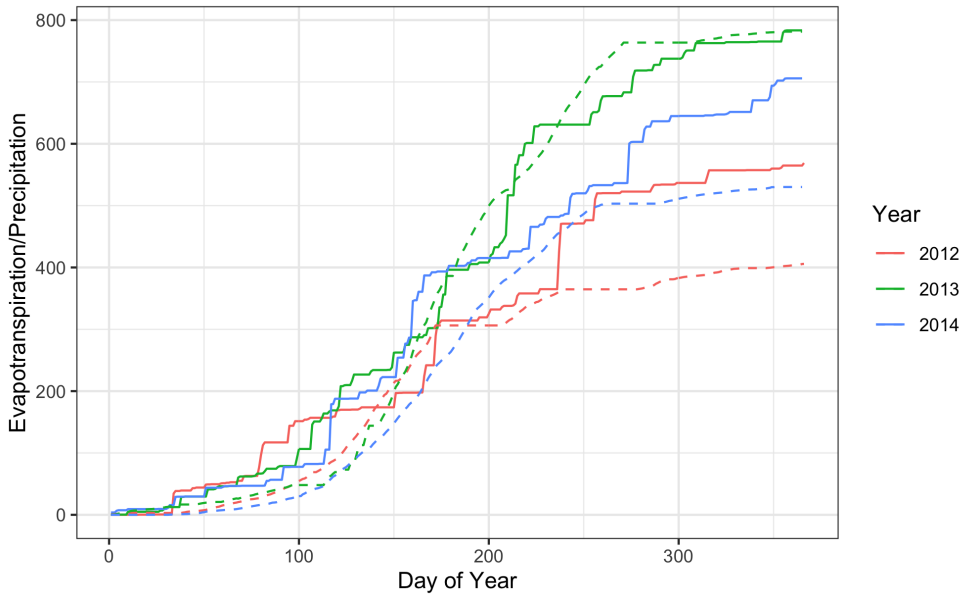

Figure 3.2: Cumulative sums of PPT [mm] (dotted) and ET [mm day^{-1}] (solid) for the years 2012 (red), 2013 (green), and 2014 (blue).

3.3.2 ET Post-Drought Response

ET is an important variable as it is how much water is evaporated from plants to the atmosphere which effects water cycle dynamics and carbon dynamics (Allen et al., 1989). For ET, we find that the total amount of evapotranspiration compared to the baseline (728.3343 mm day^{-1}), drought-year (409.7985 mm day^{-1}), and subsequent years after was higher in 2013 (781.372 mm day^{-1}) and 2014 (530.09 mm day^{-1}), shown in Table 3.2. The strong reduction in ET in 2012 (409.7985 mm day^{-1}) to the baseline demonstrates the impact that drought had on the water cycle. Furthermore, for 2013, there was a higher amount of total ET (781.372 mm day^{-1}) relative to the baseline even with lower amounts of precipitation compared to the baseline, Table 3.2. This response of ET in 2013 represents one site's post-drought characteristics as an increase total amount of ET. Furthermore, in the early growing season (Day of Year 50-180) for 2013 there was a higher amount of ET (367.5763 mm day^{-1}) compared to the baseline (299.5648 mm day^{-1}), Figure 3.3, and Table 3.3. Where in 2012, we see that for ET it's very close to the same between the baseline (difference of 0.04 mm day^{-1}). This large response of ET in the early growing season illustrates the impacts of post-drought water cycle changes for which a large

increase in ET is shown the year after drought.

Table 3.2: Cumulative sums of precipitation (PPT) [mm], evapotranspiration (ET) [mm day^{-1} and net ecosystem exchange (NEE) [μmolCO$_2$ m^{-2} s^{-1}].

Var	Baseline	2012	2013	2014
PPT	874.5	568.9	783.4	705.8
ET	728.3343	405.7975	781.372	530.09
NEE	-0.00131	-0.00031	-0.00598	-0.00256

As we saw in 2013 with an increase in total growing season ET, for 2014 it exhibited a return to the baseline early growing season totals (328.2751 mm day^{-1}), Table 3.3 and Figure 3.3. However, for the yearly totals that 2014 exhibited a smaller total for ET (530.09 mm day^{-1}) compared to the baseline (728.3343 mm day^{-1}). This may be a result from having a low amount of PPT for 2014 (705.8 mm) from the pre-drought conditions rather than being a direct response of post-drought conditions. The primary response of the water cycle conditions is in the early growing season because it has a larger response to the post-drought conditions. For the early growing season, ET decreased from 2013 (-39.3012 mm day^{-1}) and moved closer to the baseline (difference of 28.7103 mm day^{-1}). This suggests that two years post-drought the ET returns back to pre-drought conditions. This illustrates the sensitivity of ET for one site after a major drought period and its recovery time back to pre-drought conditions.

3.3.3 NEE Post-Drought Response

The drought year for KON showed an increase in annual sums for NEE of 0.001 μmolCO$_2$ m^{-2} s^{-1} from pre-drought conditions. One year after drought there was a 0.00467 μmolCO$_2$ m^{-2} s^{-1} decrease in NEE annually, Table 3.2 and Figure 3.4. Furthermore in the early spring and growing season, we see a decrease of NEE of 0.00229 μmolCO$_2$ m^{-2} s^{-1} or three times the baseline (, Figure 3.4). The large decrease within the early growing season suggests the immediate carbon response post-drought. A larger assimilation of carbon into the plants is experienced in the early growing season and throughout the year. This may suggest the plant response to

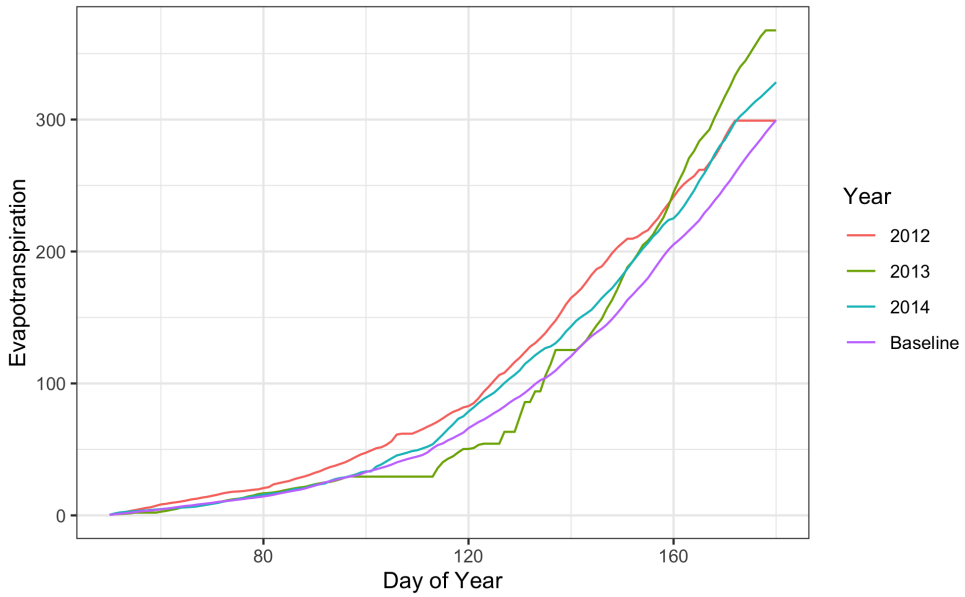

Figure 3.3: Cumulative daily sum of ET [mm day^{-1}] for early growing season (DoY 50-180). For the years 2012 (red), 2013 (green), 2014 (blue) and the baseline period (purple).

drought is to assimilate higher amounts of carbon that was potentially cut-off from the year prior with drought. The larger response (-0.00332 μmolCO$_2$ m^{-2} s^{-1}) in the early growing suggests a faster and earlier blooming season with higher amounts of carbon passing to the plants. The annual sum being nearly five times larger than the baseline period (Table 3.2) further suggests the plants initiative in assimilation higher amounts of carbon as lost a significant portion during the drought.

Table 3.3: Early growing season (DoY 50-180) sums for evapotranspiration (ET) [mm day^{-1}] and net ecosystem exchange (NEE) [μmolCO$_2$ m^{-2} s^{-1}].

Var	Baseline	2012	2013	2014
ET	299.5648	299.1525	367.5763	328.2751
NEE	-0.00103	-0.00167	-0.00332	-0.00161

For the early growing season, NEE increases from the strong 2013 year (-0.00161 μmolCO$_2$ m^{-2} s^{-1}). In 2014, the NEE response is similar to that of ET and returns to the baseline state (difference of 0.00125 μmolCO$_2$ m^{-2} s^{-1}), Table 3.2. This illustrates the carbon flux returning to its baseline state after the large deviation of NEE in 2013 (difference of 0.00171 μmolCO$_2$

m^{-2} s^{-1}). This suggests that two years after the extreme drought the amount of carbon being exchanged between this ecosystem returns back to base state. This aligns with the same time period as ET return back to base state after a strong deviation from the baseline. This further suggests that the water and carbon cycle show the same change post-drought for this specific one site case.

ET and NEE demonstrate similar responses in their post-drought recovery times. Both ET and NEE were impacted over the same period of time in returning back closely to baseline two years post extreme drought and expressing higher amounts of ET and NEE. However, there was a strong difference between the magnitudes one year post-drought. NEE had five times the amount difference of sums between the pre-drought (-0.00131 μmolCO$_2$ m^{-2} s^{-1}) state to 2013 (0.00598 μmolCO$_2$ m^{-2} s^{-1}), Table 3.2. Furthermore, in the early growing season its noted to be already three times larger than the pre-drought period. This suggests for one year post-drought cases that the carbon will receive a stronger response in magnitude to extreme drought in both annual total and early growing season.

3.4 Conclusion

There is a large impact on local water and carbon fluxes during extreme drought events. In 2012, there was a strong reduction in precipitation, evapotranspiration and net ecosystem exchange annually and early growing season. This reduction conforms to past research (Aires et al., 2008; Ghannoum, 2009; Ripley et al., 2007; Wolf et al., 2016) where they saw a reduction in these variables.

In the first year following the drought, there was an increased amount of ET and NEE annually and especially in the early growing season. This illustrates the alike responses between the local water and carbon cycles. This strong signal can be linked to ecosystem/plants response to the extreme drought case, in that the local climate experienced a much larger amount of ET and NEE the subsequent year. This demonstrates that with a strong reduction in carbon being exchanged during drought, the following year received a much larger carbon exchange

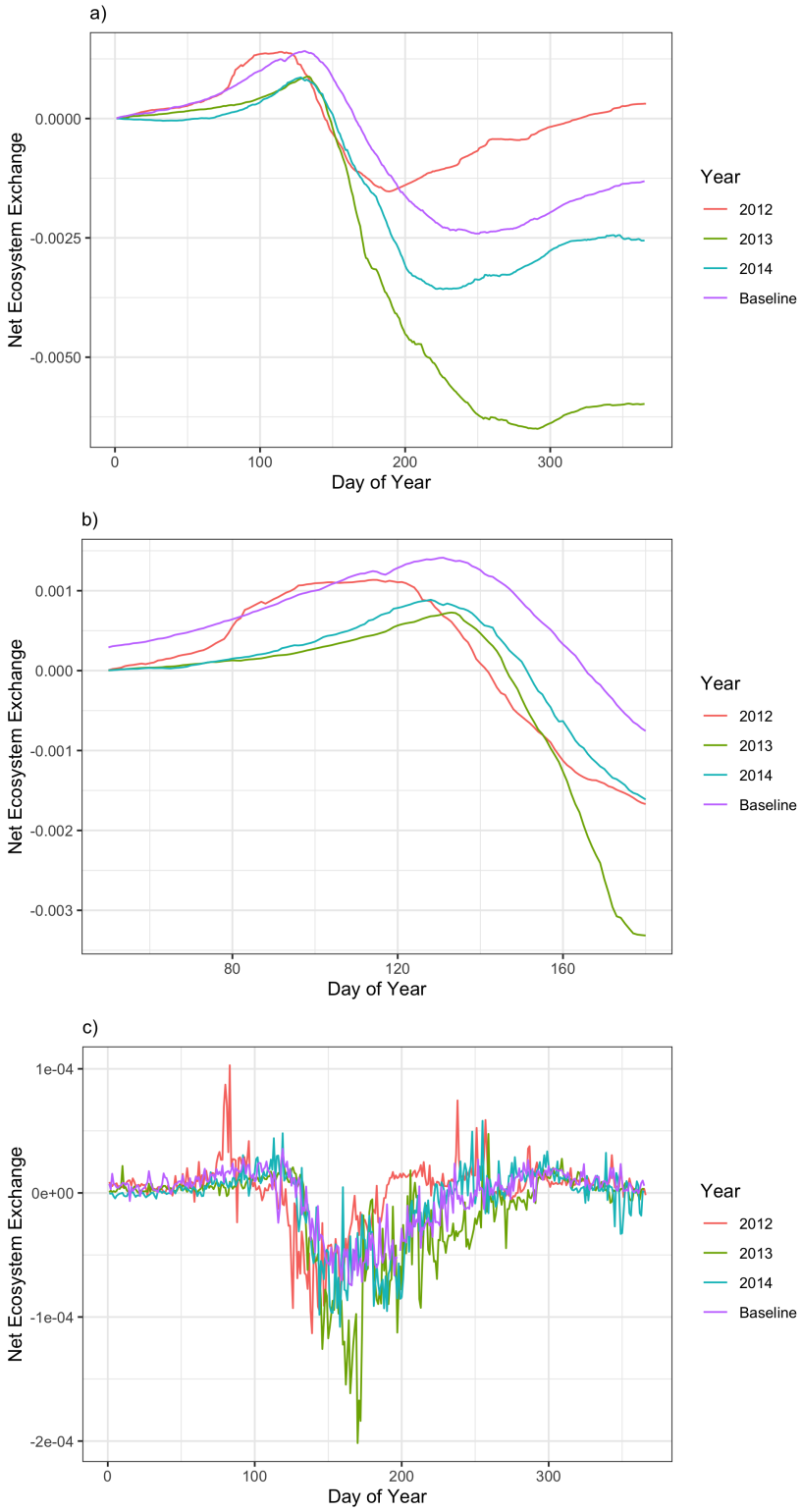

Figure 3.4: Cumulative annual sum of NEE (a) [μmolCO$_2$ m^{-2} s^{-1}], cumulative early growing season (DoY 50-180) of NEE (b), and daily average NEE (c) for the years 2012 (red), 2013 (green), 2014 (blue) and the baseline period (purple).

into the ecosystem. The following year, two years post-drought, we saw that the water and carbon fluxes start to return back to pre-drought conditions. This again suggests that it takes about two years for these ecosystems to return back to pre-drought conditions under small deviations between air temperature and vapor pressure deficit. One limitation of this study would be only analyzing one sites response for each of these variables. Further implementation of this work would stretch out to other various sites and ecosystems to see if they exhibit these characteristics.

The implications of this work shows the responses of the water and carbon fluxes during drought and how they respond to extreme drought two years prior. As global frequency and intensity of drought is projected to increase (Dai, 2013; Trenberth et al., 2014; Smith et al., 2009) it is essential to monitor and understand these impacts that drought has on these ecosystems post event. This paper demonstrates the effects that extreme drought has on the water and carbon fluxes in a C_4 cover grassland in the Central Plains.

Chapter 4

Conclusion

This research aimed to analyze the vegetation impacts on the local and regional water and carbon fluxes of Kansas grasslands. By classifying the different environments to evaluate the responses and temporal dynamics (Chapter 2) and analyzing post-drought responses the impacts (Chapter 3) from the vegetation are demonstrated. Based on the quantitative and qualitative analysis from classifying into the different environments, it can be concluded that differences in vegetation cover alter the responses of the water and carbon fluxes. Furthermore, that different global climate change conditions will alter the responses differently for each of the represented grasslands. However, the temporal dynamics of these vegetation covers indicated small variance across the different environments with one caveat being that KFB had higher coherency for environments that vegetation tended to thrive. This suggests that although the temporal dynamics of these variables will not change, the magnitudes and variance along these different classes induced by climate change will alter the feedbacks between the water and carbon fluxes. Additionally, Chapter 2 was able to illustrate that under different environmental conditions the responses of the water and carbon fluxes for these grasslands varied and experienced higher correlation and smaller variance in environments they tend to thrive in (Wang et al., 2013; Liu et al., 2015).

Chapter 3 was able to demonstrate how an extreme event, drought, impacted the local water and carbon fluxes. The year of extreme drought there was a strong reduction in precipitation, evapotranspiration and net ecosystem exchange. One year following the drought, there was an increase in evapotranspiration and net ecosystem exchange annually and in the early growing season. NEE increased five times the amount of the pre-drought period annually

and three times the amount in the early growing season, demonstrating the strong response after drought. Two years after drought ET and NEE was shown to return close to baseline pre-drought conditions suggesting a two year recovery time with extreme drought cases. This research was able to demonstrate the local water and carbon responses to an extreme drought case and focused on the post-drought magnitudes and recovery time of these variables.

Based on these conclusions and results, future studies could address the model results in Chapter 2. Since, Chapter 2 used the base parameterization scheme with NCEP forcing data, the model results with the different quantitative statistics were relatively low. Understanding the divergence of the homogeneity/heterogeneity of vegetation would be beneficial in improving model dynamics in both land-surface and climate models, instead of these models 'understanding' these processes at a site (pixel) level. Furthermore, parameterizing the heterogeneous vegetation in the model would be useful for allocating to the different water and carbon fluxes within these ecosystems. Results displayed that in implementing these models there must be some better parameterization for these different heterogeneous vegetation.

Additionally, in Chapter 3 the results only demonstrated one site's response to one extreme event case. Further research can be conducted on providing more sites (vegetation) coverage in evaluating the water and carbon variables response to extreme events. This will ensure that the results from Chapter 3 are either similar or different based on the magnitude or recovery time across each added ecosystem. This will provide further insight as to how vegetation plays a different role across each ecosystem and how it tailors to each environment. Furthermore, using different cases of drought would prove to be useful in determining the impacts that drought has on vegetation. For example, using a temporal period as a component for drought or using different defined 'droughts' could tailor responses dissimilar to Chapter 3.

These two chapters were able to present the impacts that vegetation has on the local and regional water and carbon fluxes in Kansas grasslands. By allocating to the different environments and analyzing the post-drought responses of these variables we further improve our understanding of these fluxes. This research further demonstrates how essential vegetation's

role is in altering the local climate.

References

Aires, L. M., C. A. Pio, and J. S. Pereira, 2008: The effect of drought on energy and water vapour exchange above a mediterranean C3/C4 grassland in Southern Portugal. *Agricultural and Forest Meteorology*, **148**, 565–579, doi:10.1016/j.agrformet.2007.11.001.

Al-Kaisi, M. M., R. W. Elmore, J. G. Guzman, H. M. Hanna, C. E. Hart, M. J. Helmers, E. W. Hodgson, A. W. Lenssen, A. P. Mallarino, A. E. Robertson, and J. E. Sawyer, 2013: Drought impact on crop production and the soil environment: 2012 experiences from Iowa. *Journal of Soil and Water Conservation*, **68**, 19–24, doi:10.2489/jswc.68.1.19A.

Allen, R. G., M. E. Jensen, J. L. Wright, and R. D. Burman, 1989: Operational Estimates of Reference Evapotranspiration. *Agronomy Journal*, **81**, 650–662, doi:https://doi.org/10.2134/agronj1989.00021962008100040019x.
URL `https://doi.org/10.2134/agronj1989.00021962008100040019x`

Arnone, J. A., R. L. Jasoni, A. J. Lucchesi, J. D. Larsen, E. A. Leger, R. A. Sherry, Y. Luo, D. S. Schimel, and P. S. Verburg, 2011: A climatically extreme year has large impacts on C4 species in tallgrass prairie ecosystems but only minor effects on species richness and other plant functional groups. *Journal of Ecology*, **99**, 678–688, doi:10.1111/j.1365-2745.2011.01813.x.

Barger, N. N., S. R. Archer, J. L. Campbell, C. Y. Huang, J. A. Morton, and A. K. Knapp, 2011: Woody plant proliferation in North American drylands: A synthesis of impacts on ecosystem carbon balance. *Journal of Geophysical Research: Biogeosciences*, **116**, 1–17, doi:10.1029/2010JG001506.

Betts, A. K. and J. H. Ball, 1997: Albedo over the boreal forest. *Journal of Geophysical Research Atmospheres*, **102**, 28901–28909, doi:10.1029/96jd03876.

Bonan, G. B., S. Levis, L. Kergoat, and K. W. Oleson, 2002: Landscapes as patches of plant functional types: An integrating concept for climate and ecosystem models. *Global Biogeochemical Cycles*, **16**, 5–1–5–23, doi:10.1029/2000gb001360.

Bonan, G. B., S. Levis, S. Sitch, M. Vertenstein, and K. W. Oleson, 2003: A dynamic global vegetation model for use with climate models: Concepts and description of simulated vegetation dynamics. *Global Change Biology*, **9**, 1543–1566, doi:10.1046/j.1365-2486.2003.00681.x.

Bonan, G. B., M. Williams, R. A. Fisher, and K. W. Oleson, 2014: Modeling stomatal conductance in the earth system: Linking leaf water-use efficiency and water transport along the soil-plant-atmosphere continuum. *Geoscientific Model Development*, **7**, 2193–2222, doi:10.5194/gmd-7-2193-2014.

Boyer, J. S., P. Byrne, K. G. Cassman, M. Cooper, D. Delmer, T. Greene, F. Gruis, J. Habben, N. Hausmann, N. Kenny, R. La, S. Paszkiewicz, D. Porter, A. Schlegel, J. Schussler, T. Setter, J. Shanahan, R. E. Sharp, T. J. Vyn, D. Warner, and J. Gaffney, 2013: The U.S. drought of 2012 in perspective : A call to action. *Global Food Security*, **2**, 139–143, doi:10.1016/j.gfs.2013.08.002.

Breshears, D. D., N. S. Cobb, P. M. Rich, K. P. Price, C. D. Allen, R. G. Balice, W. H. Romme, J. H. Kastens, M. L. Floyd, J. Belnap, J. J. Anderson, O. B. Myers, and C. W. Meyer, 2005: Regional vegetation die-off in response to global-change-type drought. *Proceedings of the National Academy of Sciences of the United States of America*, **102**, 15144–15148, doi:10.1073/pnas.0505734102.

Breshears, D. D., O. B. Myers, C. W. Meyer, F. J. Barnes, C. B. Zou, C. D. Allen, N. G. McDowell, and W. T. Pockman, 2009: Research communications research communications Tree die-off in response to global change-type drought: Mortality insights from a decade of plant water potential measurements. *Frontiers in Ecology and the Environment*, **7**, 185–189, doi:10.1890/080016.

Brookshire, E. N. and T. Weaver, 2015: Long-term decline in grassland productivity driven by increasing dryness. *Nature Communications*, **6**, doi:10.1038/ncomms8148.

Brunsell, N. A. and M. C. Anderson, 2011: Characterizing the multi-scale spatial structure of remotely sensed evapotranspiration with information theory. *Biogeosciences*, **8**, 2269–2280, doi:10.5194/bg-8-2269-2011.

Brunsell, N. A., J. B. Nippert, and T. L. Buck, 2014: Impacts of seasonality and surface heterogeneity on water-use efficiency in mesic grasslands. *Ecohydrology*, **7**, 1223–1233, doi:10.1002/eco.1455.

Camino-Serrano, M., B. Gielen, S. Luyssaert, and P. Ciais, 2014: Linking variability in soil solution dissolved organiccarbon to climate, soil type, and vegetation type. *Global Biogeochemical Cycles*, 1199–1214, doi:10.1002/2013GB004726.Received.

Carmo-Silva, A. E., S. J. Powers, A. J. Keys, M. C. Arrabaça, and M. A. Parry, 2008: Photorespiration in C4 grasses remains slow under drought conditions. *Plant, Cell and Environment*, **31**, 925–940, doi:10.1111/j.1365-3040.2008.01805.x.

Collatz, J. G., T. J. Ball, C. Grivet, and J. A. Berry, 1991: Physiological and environmental regulation of stomatal conductance, photosynthesis and transpiration: a model that includes a laminar boundary layer. *Agricultural and Forest Meteorology*, **54**, 107–136, doi:https://doi.org/10.1016/0168-1923(91)90002-8.
URL `https://www.sciencedirect.com/science/article/pii/0168192391900028`

Collatz, J. G., J. A. Berry, and J. S. Clark, 1998: Effects of climate and atmospheric CO(2) partial pressure on the global distribution of C(4) grasses: present, past, and future. *Oecologia*, **114**, 441–454, doi:10.1007/s004420050468.

Dai, A., 2011: Drought under global warming: a review. *WIREs Climate Change*, **2**, 45–65, doi:https://doi.org/10.1002/wcc.81.
URL `https://doi.org/10.1002/wcc.81`

— 2013: Increasing drought under global warming in observations and models. *Nature Climate Change*, **3**, 52–58, doi:10.1038/nclimate1633.

De Boeck, H. J., F. E. Dreesen, I. A. Janssens, and I. Nijs, 2010: Climatic characteristics of heat waves and their simulation in plant experiments. *Global Change Biology*, **16**, 1992–2000, doi:10.1111/j.1365-2486.2009.02049.x.

Dreesen, F. E., H. J. De Boeck, I. A. Janssens, and I. Nijs, 2012: Summer heat and drought extremes trigger unexpected changes in productivity of a temperate annual/biannual plant community. *Environmental and Experimental Botany*, **79**, 21–30, doi:10.1016/j.envexpbot.2012.01.005.
URL http://dx.doi.org/10.1016/j.envexpbot.2012.01.005

Easterling, D. R., G. A. Meehl, C. Parmesan, S. A. Changnon, T. R. Karl, and L. O. Mearns, 2000: Climate Extremes: Observations, Modeling, and Impacts. **289**, 2068–2075.

Ehleringer, J. and O. Björkman, 1977: Quantum Yields for CO(2) Uptake in C(3) and C(4) Plants: Dependence on Temperature, CO(2), and O(2) Concentration. *Plant physiology*, **59**, 86–90, doi:10.1104/pp.59.1.86.
URL http://www.ncbi.nlm.nih.gov/pubmed/16659794{%}0Ahttp://www.pubmedcentral.nih.gov/articlerender.fcgi?artid=PMC542335

Farooq, M., M. Hussain, A. Wahid, and K. H. M. Siddique, 2012: *Drought Stress in Plants: An Overview*, Springer Berlin Heidelberg, Berlin, Heidelberg. 1–33.
URL https://doi.org/10.1007/978-3-642-32653-0{_}1

Fattet, M., Y. Fu, M. Ghestem, W. Ma, M. Foulonneau, J. Nespoulous, Y. Le Bissonnais, and A. Stokes, 2011: Effects of vegetation type on soil resistance to erosion: Relationship between aggregate stability and shear strength. *Catena*, **87**, 60–69, doi:10.1016/j.catena.2011.05.006.

Fischer, E. M. and C. Schär, 2009: Future changes in daily summer temperature variabil-

ity: Driving processes and role for temperature extremes. *Climate Dynamics*, **33**, 917–935, doi:10.1007/s00382-008-0473-8.

Foley, J. A., S. Levis, and M. H. Costa, 2000: Incorporating Dynamic Vegetation Cover. *Ecological Applications*, **10**, 1620–1632.

Ghannoum, O., 2009: C4 photosynthesis and water stress. *Annals of Botany*, **103**, 635–644, doi:10.1093/aob/mcn093.

Ghannoum, O., S. von Caemmerer, and J. P. Conroy, 2002: The effect of drought on plant water use efficiency of nine NAD-ME and nine NADP-ME Australian C4 grasses. *Functional plant biology : FPB*, **29**, 1337–1348, doi:10.1071/FP02056.

Griffith, J. A., E. A. Martinko, J. K. Whistler, and K. P. Price, 2002: Interrelationships among landscapes, NDVI, and stream water quality in the U.S. Central Plains. *Ecological Applications*, **12**, 1702–1718, doi:10.1890/1051-0761(2002)012[1702:IALNAS]2.0.CO;2.

Haddad, N. M., D. Tilman, and J. M. Knops, 2002: Long-term oscillations in grassland productivity induced by drought. *Ecology Letters*, **5**, 110–120, doi:10.1046/j.1461-0248.2002.00293.x.

Hanson, P. J. and J. F. Weltzin, 2000: Drought disturbance from climate change: Response of United States forests. *Science of the Total Environment*, **262**, 205–220, doi:10.1016/S0048-9697(00)00523-4.

Heaton, E., F. Dohleman, and S. Long, 2008: Meeting US biofuel goals with less land: the potential of Miscanthus. *Global Change Biology*, **14**, 2000–2014, doi:https://doi.org/10.1111/j.1365-2486.2008.01662.x.
URL `https://doi.org/10.1111/j.1365-2486.2008.01662.x`

Heckathorn, S. A. and E. H. DeLucia, 1994: Drought-Induced Nitrogen Retranslocation in Perennial C4 Grasses of Tallgrass Prairie. *Ecology*, **75**, 1877–1886,

doi:https://doi.org/10.2307/1941592.

URL https://esajournals.onlinelibrary.wiley.com/doi/abs/10.2307/1941592

Hewitson, B. C. and R. G. Crane, 2002: Self-organizing maps: Applications to synoptic climatology. *Climate Research*, **22**, 13–26, doi:10.3354/cr022013.

Hoover, D. L., A. K. Knapp, and M. D. Smith, 2014: Resistance and resilience of a grassland ecosystem to climate extremes. *Ecology*, **95**, 2646–2656, doi:10.1890/13-2186.1.

Hufkens, K., T. F. Keenan, L. B. Flanagan, R. L. Scott, C. J. Bernacchi, E. Joo, N. A. Brunsell, J. Verfaillie, and A. D. Richardson, 2016: Productivity of North American grasslands is increased under future climate scenarios despite rising aridity. *Nature Climate Change*, **6**, 710–714, doi:10.1038/nclimate2942.

Huxman, T. E., B. P. Wilcox, D. D. Breshears, R. L. Scott, K. A. Snyder, E. E. Small, K. Hultine, W. T. Pockman, and R. B. Jackson, 2005: Ecohydrological implications of woody plant encroachment. *Ecology*, **86**, 308–319, doi:10.1890/03-0583.

Jackson, R. B., J. L. Banner, E. G. Jobbaágy, W. T. Pockman, and D. H. Wall, 2002: Ecosystem carbon loss with woody plant invasion of grasslands. *Nature*, **418**, 623–626, doi:10.1038/nature00910.

Jacobson, M. Z., 2004: The short-term cooling but long-term global warming due to biomass burning. *Journal of Climate*, **17**, 2909–2926, doi:10.1175/1520-0442(2004)017<2909:TSCBLG>2.0.CO;2.

Killi, D., F. Bussotti, A. Raschi, and M. Haworth, 2017: Adaptation to high temperature mitigates the impact of water deficit during combined heat and drought stress in C3 sunflower and C4 maize varieties with contrasting drought tolerance. *Physiologia Plantarum*, **159**, 130–147, doi:10.1111/ppl.12490.

Knapp, A. K. and M. D. Smith, 2001: Variation among biomes in temporal dynamics of aboveground primary production. *Science*, **291**, 481–484, doi:10.1126/science.291.5503.481.

Lhomme, J., A. Chehbouni, and B. Monteny, 1994: Effective Parameters of Surface Energy Balance in Hetereogenous Landscape, 297–309.

Liu, P. C., 1994: Wavelet Spectrum Analysis and Ocean Wind Waves. *Wavelets in Geophysics*, E. Foufoula-Georgiou and P. Kumar, eds., Academic Press, volume 4 of *Wavelet Analysis and Its Applications*, 151–166.
URL https://www.sciencedirect.com/science/article/pii/B9780080520872500128

Liu, X., Y. Bo, J. Zhang, and Y. He, 2015: Classification of C3 and C4 vegetation types using MODIS and ETM+ blended high spatio-temporal resolution data. *Remote Sensing*, **7**, 15244–15268, doi:10.3390/rs71115244.

Logan, K. E. and N. A. Brunsell, 2015: Influence of drought on growing season carbon and water cycling with changing land cover. *Agricultural and Forest Meteorology*, **213**, 217–225, doi:10.1016/j.agrformet.2015.07.002.
URL http://dx.doi.org/10.1016/j.agrformet.2015.07.002

Manzoni, S., G. Vico, G. Katul, P. A. Fay, W. Polley, S. Palmroth, and A. Porporato, 2011: Optimizing stomatal conductance for maximum carbon gain under water stress: A meta-analysis across plant functional types and climates. *Functional Ecology*, **25**, 456–467, doi:10.1111/j.1365-2435.2010.01822.x.

Meir, P., D. B. Metcalfe, A. C. Costa, and R. A. Fisher, 2008: The fate of assimilated carbon during drought: Impacts on respiration in Amazon rainforests. *Philosophical Transactions of the Royal Society B: Biological Sciences*, **363**, 1849–1855, doi:10.1098/rstb.2007.0021.

Niu, G. Y., Z. L. Yang, K. E. Mitchell, F. Chen, M. B. Ek, M. Barlage, A. Kumar, K. Manning, D. Niyogi, E. Rosero, M. Tewari, and Y. Xia, 2011: The community Noah land surface

model with multiparameterization options (Noah-MP): 1. Model description and evaluation with local-scale measurements. *Journal of Geophysical Research Atmospheres*, **116**, 1–19, doi:10.1029/2010JD015139.

Notaro, M., Z. Liu, and J. W. Williams, 2006: Observed vegetation - Climate feedbacks in the United States. *Journal of Climate*, **19**, 763–786, doi:10.1175/JCLI3657.1.

Pielke, R. A., J. Adegoke, A. Beltrán-Przekurat, C. A. Hiemstra, J. Lin, U. S. Nair, D. Niyogi, and T. E. Nobis, 2007: An overview of regional land-use and land-cover impacts on rainfall. *Tellus, Series B: Chemical and Physical Meteorology*, **59**, 587–601, doi:10.1111/j.1600-0889.2007.00251.x.

Quideau, S. A., O. A. Chadwick, A. Benesi, R. C. Graham, and M. A. Anderson, 2001: A direct link between forest vegetation type and soil organic matter composition. *Geoderma*, **104**, 41–60, doi:10.1016/S0016-7061(01)00055-6.

Randerson, J. T., G. R. van der Werf, G. J. Collatz, L. Giglio, C. J. Still, P. Kasibhatla, J. B. Miller, J. W. White, R. S. DeFries, and E. S. Kasischke, 2005: Fire emissions from C3 and C4 vegetation and their influence on interannual variability of atmospheric CO2 and δ13CO2. *Global Biogeochemical Cycles*, **19**, 1–13, doi:10.1029/2004GB002366.

Ratajczak, Z., J. B. Nippert, and S. L. Collins, 2012: Woody encroachment decreases diversity across North American grasslands and savannas. **93**, 697–703.

Ratajczak, Z., J. B. Nippert, J. C. Hartman, and T. W. Ocheltree, 2011: Positive feedbacks amplify rates of woody encroachment in mesic tallgrass prairie. *Ecosphere*, **2**, doi:10.1890/ES11-00212.1.

Raupach, M. R. and J. J. Finnigan, 1995: Scale issues in boundary-layer meteorology: Surface energy balances in heterogeneous terrain. *Hydrological Processes*, **9**, 589–612, doi:10.1002/hyp.3360090509.

Reichstein, M., E. Falge, D. Baldocchi, D. Papale, M. Aubinet, P. Berbigier, C. Bernhofer, N. Buchmann, T. Gilmanov, A. Granier, T. Grünwald, K. Havránková, H. Ilvesniemi, D. Janous, A. Knohl, T. Laurila, A. Lohila, D. Loustau, G. Matteucci, T. Meyers, F. Miglietta, J. M. Ourcival, J. Pumpanen, S. Rambal, E. Rotenberg, M. Sanz, J. Tenhunen, G. Seufert, F. Vaccari, T. Vesala, D. Yakir, and R. Valentini, 2005: On the separation of net ecosystem exchange into assimilation and ecosystem respiration: Review and improved algorithm. *Global Change Biology*, **11**, 1424–1439, doi:10.1111/j.1365-2486.2005.001002.x.

Ricotta, C., B. C. Reed, and L. T. Tieszen, 2003: The role of C3 and C4 grasses to interannual variability in remotely sensed ecosystem performance over the US Great Plains. *International Journal of Remote Sensing*, **24**, 4421–4431, doi:10.1080/0143116031000070454.
URL https://doi.org/10.1080/0143116031000070454

Ripley, B., K. Frole, and M. Gilbert, 2010: Differences in drought sensitivities and photosynthetic limitations between co-occurring C3 and C4 (NADP-ME) Panicoid grasses. *Annals of Botany*, **105**, 493–503, doi:10.1093/aob/mcp307.

Ripley, B. S., M. E. Gilbert, D. G. Ibrahim, and C. P. Osborne, 2007: Drought constraints on C4 photosynthesis: Stomatal and metabolic limitations in C3 and C4 subspecies of Alloteropsis semialata. *Journal of Experimental Botany*, **58**, 1351–1363, doi:10.1093/jxb/erl302.

Rippey, B. R., 2015: The U.S. drought of 2012. *Weather and Cimate Extremes*, **10**, 57–64, doi:10.1016/j.wace.2015.10.004.

Rösch, A. and H. Schmidbauer, 2018: WaveletComp: Computational Wavelet Analysis. R package version 1.1., 1–38.
URL http://www.hs-stat.com/projects/WaveletComp/WaveletComp{_}guided{_}tour.pdf{%}0Ahttps://cran.r-project.org/package=WaveletComp

Ruehr, N. K., R. Grote, S. Mayr, and A. Arneth, 2019: Beyond the extreme: recovery of carbon and water relations in woody plants following heat and drought stress. *Tree Physiology*, **39**,

1285–1299, doi:10.1093/treephys/tpz032.
URL https://doi.org/10.1093/treephys/tpz032

Sage, R. F., 2004: The evolution of C4 photosynthesis. *New Phytologist*, **161**, 341–370, doi:https://doi.org/10.1111/j.1469-8137.2004.00974.x.
URL https://nph.onlinelibrary.wiley.com/doi/abs/10.1111/j.1469-8137.2004.00974.x

Sage, R. F. and D. S. Kubien, 2007: The temperature response of C3 and C4 photosynthesis. *Plant, Cell and Environment*, **30**, 1086–1106, doi:10.1111/j.1365-3040.2007.01682.x.

Schmid, H. P., 2002: Footprint modeling for vegetation atmosphere exchange studies: A review and perspective. *Agricultural and Forest Meteorology*, **113**, 159–183, doi:10.1016/S0168-1923(02)00107-7.

Scott, R. L., T. E. Huxman, D. G. Williams, and D. C. Goodrich, 2006: Ecohydrological impacts of woody-plant encroachment: Seasonal patterns of water and carbon dioxide exchange within a semiarid riparian environment. *Global Change Biology*, **12**, 311–324, doi:10.1111/j.1365-2486.2005.01093.x.

Shi, Z., M. L. Thomey, W. Mowll, M. Litvak, N. A. Brunsell, S. L. Collins, W. T. Pockman, M. D. Smith, A. K. Knapp, and Y. Luo, 2014: Differential effects of extreme drought on production and respiration: Synthesis and modeling analysis. *Biogeosciences*, **11**, 621–633, doi:10.5194/bg-11-621-2014.

Sitch, S., B. Smith, I. C. Prentice, A. Arneth, A. Bondeau, W. Cramer, J. O. Kaplan, S. Levis, W. Lucht, M. T. Sykes, K. Thonicke, and S. Venevsky, 2003: Evaluation of ecosystem dynamics, plant geography and terrestrial carbon cycling in the LPJ dynamic global vegetation model. *Global Change Biology*, **9**, 161–185, doi:10.1046/j.1365-2486.2003.00569.x.

Smith, F. A. and K. H. Freeman, 2006: Influence of physiology and climate on δD of leaf

wax n-alkanes from C3 and C4 grasses. *Geochimica et Cosmochimica Acta*, **70**, 1172–1187, doi:10.1016/j.gca.2005.11.006.

Smith, M. D., A. K. Knapp, and S. L. Collins, 2009: A framework for assessing ecosystem dynamics in response to chronic resource alterations induced by climate chnage. *Ecology*, **90**, 3279–3289.

Still, C. J., J. A. Berry, M. Ribas-Carbo, and B. R. Helliker, 2003: The contribution of C3 and C4 plants to the carbon cycle of a tallgrass prairie: An isotopic approach. *Oecologia*, **136**, 347–359, doi:10.1007/s00442-003-1274-8.

Sud, Y., J. Shukla, and Y. Mintz, 1988: Influence of Land Surface Roughness on Atmospheric Circulation and Precipitation: A Sensitivity Study with a General Circulation Model. *Applied Meteorology and Climatology*, **27**, 1036–1054.
URL https://doi.org/10.1175/1520-0450(1988)027{%}3C1036:IOLSRO{%}3E2.0.CO;2

Swann, A. L. S., 2018: Plants and Drought in a Changing Climate. *Current Climate Change Reports*, **4**, 192–201, doi:10.1007/s40641-018-0097-y.
URL https://doi.org/10.1007/s40641-018-0097-y

Syphard, A. D., T. Sheehan, H. Rustigian-Romsos, and K. Ferschweiler, 2018: Mapping future fire probability under climate change: Does vegetation matter? *PLoS ONE*, **13**, 1–23, doi:10.1371/journal.pone.0201680.

Taub, D. R., 2000: Climate and the U.S. distribution of C4 grass subfamilies and decarboxylation variants of C4 photosynthesis. *American journal of botany*, **87**, 1211–1215.

Taylor, S. H., S. P. Hulme, M. Rees, B. S. Ripley, F. Ian Woodward, and C. P. Osborne, 2010: Ecophysiological traits in C3 and C4 grasses: A phylogenetically controlled screening experiment. *New Phytologist*, **185**, 780–791, doi:10.1111/j.1469-8137.2009.03102.x.

Taylor, S. H., B. S. Ripley, F. I. Woodward, and C. P. Osborne, 2011: Drought limitation of photosynthesis differs between C3 and C4 grass species in a comparative experiment. *Plant, Cell and Environment*, **34**, 65–75, doi:10.1111/j.1365-3040.2010.02226.x.

Teuling, A. J., S. I. Seneviratne, R. Stöckli, M. Reichstein, E. Moors, P. Ciais, S. Luyssaert, B. Van Den Hurk, C. Ammann, C. Bernhofer, E. Dellwik, D. Gianelle, B. Gielen, T. Grünwald, K. Klumpp, L. Montagnani, C. Moureaux, M. Sottocornola, and G. Wohlfahrt, 2010: Contrasting response of European forest and grassland energy exchange to heatwaves. *Nature Geoscience*, **3**, 722–727, doi:10.1038/ngeo950.
URL http://dx.doi.org/10.1038/ngeo950

Thonicke, K., S. Venevsky, S. Sitch, and W. Cramer, 2001: The role of fire disturbance for global vegetation dynamics: Coupling fire into a dynamic global vegetation model. *Global Ecology and Biogeography*, **10**, 661–677, doi:10.1046/j.1466-822X.2001.00175.x.

Trenberth, K. E., A. Dai, G. Van Der Schrier, P. D. Jones, J. Barichivich, K. R. Briffa, and J. Sheffield, 2014: Global warming and changes in drought. *Nature Climate Change*, **4**, 17–22, doi:10.1038/nclimate2067.

Van der Molen, M. K., A. J. Dolman, P. Ciais, T. Eglin, N. Gobron, B. E. Law, P. Meir, W. Peters, O. L. Phillips, M. Reichstein, T. Chen, S. C. Dekker, M. Doubková, M. A. Friedl, M. Jung, B. J. van den Hurk, R. A. de Jeu, B. Kruijt, T. Ohta, K. T. Rebel, S. Plummer, S. I. Seneviratne, S. Sitch, A. J. Teuling, G. R. van der Werf, and G. Wang, 2011: Drought and ecosystem carbon cycling. *Agricultural and Forest Meteorology*, **151**, 765–773, doi:10.1016/j.agrformet.2011.01.018.
URL http://dx.doi.org/10.1016/j.agrformet.2011.01.018

Vanaja, M., S. K. Yadav, G. Archana, N. J. Jyothi Lakshmi, P. R. Ram Reddy, P. Vagheera, S. A. Abdul Razak, M. Maheswari, and B. Venkateswarlu, 2011: Response of C4 (maize) and C3 (sunflower) crop plants to drought stress and enhanced carbon dioxide concentration. *Plant, Soil and Environment*, **57**, 207–215, doi:10.17221/346/2010-pse.

Vicente-Serrano, S. M., 2007: Evaluating the impact of drought using remote sensing in a Mediterranean, Semi-arid Region. *Natural Hazards*, **40**, 173–208, doi:10.1007/s11069-006-0009-7.

Vidale, P. L., D. Lüthi, R. Wegmann, and C. Schär, 2007: European summer climate variability in a heterogeneous multi-model ensemble. *Climatic Change*, **81**, 209–232, doi:10.1007/s10584-006-9218-z.

von Fischer, J. C., L. L. Tieszen, and D. S. Schimel, 2008: Climate controls on C3 vs. C4 productivity in North American grasslands from carbon isotope composition of soil organic matter. *Global Change Biology*, **14**, 1141–1155, doi:10.1111/j.1365-2486.2008.01552.x.

Wagle, P. and P. H. Gowda, 2018: Tallgrass prairie responses to management practices and disturbances: A review. *Agronomy*, **8**, doi:10.3390/agronomy8120300.

Wang, C., E. R. Hunt, L. Zhang, and H. Guo, 2013: Phenology-assisted classification of C3 and C4 grasses in the U.S. Great Plains and their climate dependency with MODIS time series. *Remote Sensing of Environment*, **138**, 90–101, doi:10.1016/j.rse.2013.07.025.

Way, D. A., G. G. Katul, S. Manzoni, and G. Vico, 2014: Increasing water use efficiency along the C3 to C4 evolutionary pathway: A stomatal optimization perspective. *Journal of Experimental Botany*, **65**, 3683–3693, doi:10.1093/jxb/eru205.

Wehrens, R. and L. Buydens, 2007: Self- and Super-organizing Maps in R: The kohonen Package. *Wiley Interdisciplinary Reviews: Computational Statistics*, doi:10.1002/wics.10.

Wehrens, R. and J. Kruisselbrink, 2018: Flexible Self-Organizing Maps in kohonen 3.0. *Statistical Software*, **87**, doi:10.18637/jss.v087.i07.

Weltzin, J. F., M. E. Loik, S. Schwinning, D. G. Williams, P. A. Fay, B. M. Haddad, J. Harte, T. E. Huxman, A. K. Knapp, G. Lin, W. T. Pockman, M. R. Shaw, E. E. Small, M. D. Smith,

S. D. Smith, D. T. Tissue, and J. C. Zak, 2003: Assessing the Response of Terrestrial Ecosystems to Potential Changes in Precipitation. *BioScience*, **53**, 941–952, doi:10.1641/0006-3568(2003)053[0941:ATROTE]2.0.CO;2.

Williams, C. A. and J. D. Albertson, 2005: Contrasting short- and long-timescale effects of vegetation dynamics on water and carbon fluxes in water-limited ecosystems. *Water Resources Research*, **41**, 1–13, doi:10.1029/2004WR003750.

Wittmer, M., K. Auerswald, Y. Bai, R. Schäufele, and H. Schnyder, 2010: Changes in the abundance of C3/C4 species of Inner Mongolia grassland: Evidence from isotopic composition of soil and vegetation. *Global Change Biology*, **16**, 605–616, doi:10.1111/j.1365-2486.2009.02033.x.

Wolf, S., W. Eugster, C. Ammann, M. Häni, S. Zielis, R. Hiller, J. Stieger, D. Imer, L. Merbold, and N. Buchmann, 2014: Contrasting response of grassland versus forest carbon and water fluxes to spring drought in Switzerland. *Environmental Research Letters*, **9**, doi:10.1088/1748-9326/9/8/089501.

Wolf, S., T. F. Keenan, J. B. Fisher, D. D. Baldocchi, A. R. Desai, A. D. Richardson, R. L. Scott, B. E. Law, M. E. Litvak, N. A. Brunsell, W. Peters, and I. T. Van Der Laan-Luijkx, 2016: Warm spring reduced carbon cycle impact of the 2012 US summer drought. *Proceedings of the National Academy of Sciences of the United States of America*, **113**, 5880–5885, doi:10.1073/pnas.1519620113.

Wynn, J. G. and M. I. Bird, 2007: C4-derived soil organic carbon decomposes faster than its C3 counterpart in mixed C3/C4 soils. *Global Change Biology*, **13**, 2206–2217, doi:10.1111/j.1365-2486.2007.01435.x.

Yang, Z. L., G. Y. Niu, K. E. Mitchell, F. Chen, M. B. Ek, M. Barlage, L. Longuevergne, K. Manning, D. Niyogi, M. Tewari, and Y. Xia, 2011: The community Noah land surface model with

multiparameterization options (Noah-MP): 2. Evaluation over global river basins. *Journal of Geophysical Research Atmospheres*, **116**, 1–16, doi:10.1029/2010JD015140.

Yin, J. and T. L. Bauerle, 2017: A global analysis of plant recovery performance from water stress. *Oikos*, **126**, 1377–1388, doi:https://doi.org/10.1111/oik.04534.
URL https://doi.org/10.1111/oik.04534